Quasicrystals. I. Definition and structure

Dov Levine and Paul J. Steinhardt
Department of Physics, University of Pennsylvania, Philadelphia, Pennsylvania 19104-6396
(Received 3 September 1985)

In a recent paper, we introduced the concept of quasicrystals [Phys. Rev. Lett. 53, 2477 (1984)], a new class of ordered atomic structures. Quasicrystals have long-range quasiperiodic translational order and long-range orientational order. In the present paper and the following one, we discuss the details of our analysis of the mathematical and structural properties of quasicrystals. We begin with a general overview of our analysis. We then discuss our computation of the diffraction pattern of a quasilattice, using as an example the case of icosahedral orientational symmetry. We demonstrate that two quasilattices with the same orientational symmetry and quasiperiodicity which are not locally isomorphic will have diffraction patterns with different peak intensities. Finally, we describe some examples of computer modeling of atomic quasicrystals.

I. INTRODUCTION

Traditionally, the atomic structures of pure solids have been divided into two classes: crystal structures and glassy structures. Crystal structures are highly ordered: (1) They have long-range translational order characterized by a periodic spacing of unit cells; (2) they have long-range (near-neighbor bond) orientational order with a symmetry corresponding to special *crystallographic*[1] discrete subgroups of the rotation group [as represented by the 5 two-dimensional (2D) and 14 three-dimensional (3D) Bravais lattices];[2,3] and (3) they have a rotational point symmetry (also restricted to special crystallographic discrete subgroups). A glassy structure, by contrast, has none of the long-range correlations of the crystal. A metallic glass, for example, is modeled by spheres that are densely but randomly packed together.[4]

Recently, we introduced the notion of a new kind of ordered atomic structure—one which would represent a new phase of solid matter if found in nature.[5] The new structure is like a crystal in that it has long-range translational order and long-range orientational order. However, the translational order is *not* periodic and the structure does not have a rotational point symmetry. Instead, the new structure is *quasiperiodic*, a well-defined but more subtle kind of translational order. Because the new structures have many of the properties of crystals, with the notable exception that they are quasiperiodic rather than periodic, we termed them *quasiperiodic crystals*, or *quasicrystals* for short. We briefly discussed methods of constructing quasilattices and packings of the unit cells and described some of the mathematical properties of quasicrystal structures.

We also suggested that the recently reported "icosahedral phase" of aluminum manganese (*I*-Al-Mn) and related rapidly quenched alloys[6] may, in fact, be an icosahedral quasicrystal, based on a comparison of our theoretical (computed) diffraction pattern with the experimentally observed pattern.[5]

Numerous papers have appeared which discuss alternative models for the icosahedral phases of aluminum—translational-metal alloys. Some of these attempt to explain the experimental observations in terms of ordinary crystallography (e.g., multiple twinning or large unit cells or a combination of the two).[7–9] These are conceptually and, ultimately, experimentally distinguishable from our quasicrystal model; experimental investigations will eventually determine which model is correct.

In addition, there are now several different descriptions of the same quasicrystal models discussed in Ref. 5. Kramer and Neri,[10] working independently, employed a technique based on projections from a higher-dimensional periodic lattice for obtaining quasicrystal packings of unit cells. Another independent projection technique has since been found by Elser,[11] Kalugin *et al.*,[12] and Duneau and Katz.[13] We also note that the models of "amorphous structures" suggested earlier by Mercier and Levy[14] appear to be generated by yet another projection approach and probably correspond to quasicrystal structures. A number of groups[12,15–18] have discussed a density-wave description for icosahedral quasicrystals. Finally, there are the quasicrystal models obtained by the "generalized dual method"[19] (GDM) or multigrid[20] methods. These models are experimentally indistinguishable. In the present paper (hereafter referred to as I) and the following one[22] (hereafter referred to as II), we shall point to some of the advantages of the different descriptions, especially the GDM, in understanding various physical and mathematical properties of quasicrystals.

The goal of papers I and II is to explain in greater detail our theory of quasicrystal structures, as introduced in Ref. 5, and to present many new results of mathematical and physical interest.

We have divided the text into two papers. Paper I is intended as a general guide to the definition and diffraction properties of quasicrystals. We begin in Sec. II with a pedagogical overview of our analysis of quasicrystal structures. We discuss the definition of quasicrystals and how ideal quasicrystal structures can be constructed with arbitrary orientational symmetry. We generalize the notion of quasicrystals given in Ref. 5 to include any structures that are composed of unit cells and that exhibit long-range

quasiperiodic translational order and long-range orientational order, without the requirement that they be self-similar.

For the remainder of the paper we restrict our attention to the special cases of pentagonal and icosahedral quasicrystals. These are examples of the class of quasicrystals which are self-similar. We find this class to be of special interest for several reasons; (a) the class includes the simplest and most symmetrical quasicrystal structures; (b) due to their symmetries, the quasicrystals in this class have additional fascinating mathematical properties; and (c) *I*-Al-Mn (and related alloys) appears to correspond to an icosahedral quasicrystal.

In Sec. III we discuss the computation of the diffraction pattern for the 1D and 3D icosahedral quasilattice. We compare the computations for the icosahedral quasilattice with the experimentally observed electron[6,23] diffraction patterns of *I*-Al-Mn. In Sec. IV we discuss the further subdivision of quasicrystal structures of given orientational symmetry and quasiperiodicity into local isomorphism (LI) classes. Two quasicrystals are in the same LI class if and only if every finite configuration of unit cells in each occurs in the other. We argue that structures in different LI classes have different diffraction peak intensities and free energies, so that, although the ground state is degenerate, all ground-state configurations correspond to a single LI class. In Sec. V we discuss some results from our computer modeling of 2D atomic and polyball systems as an attempt to study conditions under which the formation of quasicrystal structures is energetically favorable.

Paper II is a more formal treatment of pentagonal and icosahedral quasicrystals, emphasizing methods of construction and local isomorphism properties. We discuss various methods of generating quasicrystals in one, two, and three dimensions. We show that, in addition to generating quasicrystals with arbitrary orientational symmetry, the GDM, for any fixed orientational symmetry, generates the largest set of LI classes compared to the other known construction methods. We then focus on a very special LI class of icosahedral quasicrystals for which there exist a set of "matching rules" for the unit cells, analogous to the special LI class of pentagonal quasicrystal tilings found by Penrose.[24] The matching rules determine how two unit cells may be packed together and are designed so that the cells are forced to pack into icosahedral quasicrystal structures (without matching rules, the unit cells can be packed periodically or quasiperiodically). These matching rules might be physically effected in some systems through local interactions of atoms or clusters of atoms.

II. GENERAL OVERVIEW

A. Motivation

In a study directed towards understanding the structural properties of supercooled liquids and glassy solids, Steinhardt *et al.*[25] found extended (but finite range) icosahedral orientational order in computer simulations of supercooled liquids which suggested that they attain a surprising degree of icosahedral orientational order before glassification. Two distinct theoretical efforts have arisen from attempts to assess the significance of the observed orientational order. One approach, pursued by several groups,[26] is based on the notion that a metallic glass may be described as a state with extended (but finite range) icosahedral orientational order and entangled icosahedral disclination defects. The "ideal" glass state would be one in which the defects were ordered so as to form a crystal with a large unit cell—a Frank-Kasper phase.[27] A second approach, pursued by the authors, is to consider the possibility that the "ideal glass" might have *infinite* range icosahedral orientational order.[28] The notion is that perhaps such a state may be a locally (or even globally) stable state of matter, but difficult to obtain due to kinetic considerations. A rapidly quenched liquid might begin to form such a state but fall out of thermal equilibrium and form a "real glass" before ever reaching the ideal state. The chief stumbling block to this approach was that it was not known how to construct a perfect icosahedrally oriented dense structure. The prejudice, in fact, was that such a structure could not exist because icosahedra do not pack crystallographically; the geometric frustration induced by the demand for icosahedral order would severely limit the range over which such order could persist. We will comment further on the relationship between these two approaches to understanding glass structure in the conclusions, Sec. VI.

Our study of the "nonperiodic" tilings discovered by Penrose[24,29] suggested that the stumbling block might be surmountable. The tilings have long-range pentagonal orientational order, even though pentagons cannot pack crystallographically. We proceeded to construct and analyze a three-dimensional analogue with icosahedral symmetry.

In the process, we found that the Penrose tilings (and the icosahedral analogue) not only have long-range orientational order, but also have long-range 2D (or 3D) quasiperiodic translational order. Once the true symmetries of the structures had been identified, an analysis of the physical properties (e.g., diffraction pattern, elasticity theory, etc.) became possible. Because the symmetries are fundamentally different from those of crystals or glasses, it became apparent that atomic configurations corresponding to such new structures would represent a new phase of solid matter if found in nature. The new quasiperiodic structures were termed "quasicrystals." We initiated a series of computer simulations to find conditions under which quasicrystal configurations of atoms are locally, and perhaps globally, stable (see Sec. V).

In 1984, Shechtman *et al.*[6] reported an alloy of aluminum and manganese which apparently possesses icosahedral symmetry. The electron diffraction pattern of the new alloy corresponded very closely with our computations of the diffraction pattern for an icosahedral quasicrystal. The correspondence led us to suggest that the Al-Mn alloy may be an example of an icosahedral quasicrystal. A brief summary of our analysis and a comparison with experiment was presented in Ref. 5.

Although at present quasicrystals with only icosahedral,[6] dodecagonal[30] and decagonal[31] symmetry

have been reported, we are hopeful that, now that attention has been focused on this new class of ordered atomic structures, many more examples will be found. In that case, the symmetry possibilities and theoretical notions introduced in these papers may have further physical significance.

B. Basic definitions

An ideal quasicrystal is constructed by the infinite repetition in space of two or more distinct (atomic or molecular) structural units, called "unit cells," packed in a lattice that has long-range quasiperiodic translational order and long-range orientational order. By a quasicrystal unit cell, we mean only a repeating motif, but, unlike crystals, the motif is not repeated periodically. We will refer to the structure obtained by a packing of unit cells (e.g., as defined by the vertices of the cells) as a *packing* in general, a *tiling* for the special case of two dimensions. The underlying lattice will be referred to as a *quasilattice*. The term *quasicrystal* will refer to the physical (atomic or molecular) structure, corresponding to some atomic decoration of the unit cells, or its ideal mathematical abstraction (where the atoms are replaced by points).

The formal properties of quasicrystals are as follows.

(a) *Orientational order*: The bond angles between neighboring atoms or clusters (measured with respect to some fixed set of axes) have long-range correlations and are oriented, on the average, along a set of "star" axes that define the orientational order. For the quasicrystal packings we shall describe, each edge of each unit cell in the packing is oriented along one of the set of orientational star axes; this clearly establishes the fact that the structure has perfect long-range orientational order. The set of star axes can be chosen arbitrarily, in general.

Quasiperiodic structures formed for a set of star axes which correspond to a *crystallographic* orientational symmetry have been known for a long time and are normally referred to as "incommensurate crystals."[32] Quasicrystals represent the generalization to quasiperiodic structures with *noncrystallographic* orientational symmetry (e.g., decagonal orientational order in two dimensions and icosahedral orientational order in three dimensions). We shall mention in Sec. II F some important physical distinctions between incommensurate crystals and quasicrystals with noncrystallographic symmetries.

(b) *Minimal separation between atomic sites*: There exist distances r and R (both greater than zero) such that the separation between any two nearest-neighbor sites lies between r and R.[33] This distinguishes the quasicrystal from a set of sites obtained by superimposing two periodic lattices with periods whose ratio is irrational, in which case the spacing between neighboring lattice points can be arbitrarily small. In particular, minimal separation is a necessary condition for the structure to be defined in terms of a finite number of fundamental unit cells.

(c) *Quasiperiodic translational order*: The (mass) density function of the quasicrystal is quasiperiodic. A function is quasiperiodic if it can be expressed as a sum of periodic functions with periods, where at least some of the periods are incommensurate (i.e., their ratio is irrational).[34] (Some may wish to distinguish between quasiperiodic, where there is only a finite sum of functions, and almost periodic, where there is an infinite sum of functions; we make no such distinction in papers I and II.) For example, the function

$$f(x)=\cos(x)+\cos(\pi x)$$

is quasiperiodic. The quasiperiodicity is characterized by special sets of irrational numbers. The set of irrational numbers is constrained by the orientational symmetry whenever that symmetry is noncrystallographic. Therefore, we find it useful to classify quasicrystals both by their orientational symmetry and their quasiperiodicity.

It should be added that there is no nontrivial translation of either the quasilattice or the packing that leaves them invariant, and there is no rotational point symmetry. In fact, outside of certain exceptional cases, there is no center of symmetry in the quasicrystal.[35]

In our original research,[5] we were interested in space-filling structures which, in addition to having properties (a)—(c), are also self-similar. According to our conjecture,[5,36] self-similar quasicrystals can be constructed with orientational symmetry corresponding to any polygon in two dimensions or polyhedron in three dimensions. We will discuss examples of self-similarity transformations or *deflation rules* in paper II.

More recently,[19,21] the GDM was used to demonstrate that it is possible to produce a packing in two or three dimensions from a finite number of unit cells such that the tiling has perfect long-range quasiperiodic translational order and perfect long-range orientational alignments along an *arbitrary* set of star vectors. For an arbitrary set of star vectors without a high degree of orientational symmetry, the associated quasicrystal packing is not self-similar. We think it is natural to broaden our definition of "quasicrystal" to include these more general quasiperiodic packings.

C. Generalized dual method

Several methods have been found for generating quasicrystal packings of unit cells. A technique which we recently discussed (it is an application of the ideas of de Bruijn[20] and Kramer and Neri[10] to the most general N-grids) is called the *generalized dual method* or GDM. This method is a straightforward approach for obtaining quasicrystal packings with arbitrary orientational symmetry.

In order to discuss the GDM, it is useful to establish the definitions of a few terms.

(1) A *grid* is any countably infinite set of infinite (unbounded) nonintersecting curves in two dimensions or surfaces in three dimensions. In two dimensions, an *N-grid* is a set of N grids such that each curve in the ith grid intersects each curve in the jth at exactly one point for each $i\neq j$. In three dimensions, an N-grid is a set of N grids such that any triplet of surfaces in the ith, jth, and kth grids, respectively (for $i\neq j\neq k$), intersect at exactly one point. Associated with a grid is a star vector, $\mathbf{e}_i$, which plays an important role in the dual construction.

(2) A *quasilattice* is a set of points lying at the intersec-

tion of a special class of N-grids which have the following three properties: (a) quasiperiodic translational symmetry, (b) orientational symmetry, and (c) a finite number of Voronoi cell shapes. [A Voronoi cell, known also as the Wigner-Seitz or Dirichlet cell, can be associated with each point in the quasilattice and is the convex polygon (polyhedron) whose edges (faces) are determined by constructing all lines (planes) that bisect the line segments joining the point to its neighbors.[3]] Condition (c) automatically insures that the special class of N-grids satisfy the minimal separation condition defined in Sec. II B. The Ammann quasilattice, to be described in Sec. II D, corresponds to a 5-grid that satisfies these conditions. An example of an N-grid that fails to meet the three conditions is one formed from five periodically spaced grids oriented normal to the five symmetry axes of a pentagon; in particular, the intersections points do not satisfy condition (c).

For an arbitrary N-grid, each grid curve (or surface) can be indexed by an integer corresponding to its ordinal position in the grid (the star vector, $\mathbf{e}_i$, associated with each grid determines the positive ordinal direction). Each open region between grid lines (or planes) is characterized by N integers, k_i: For each $i \leq N$, an open region lies between the grid curves (or surfaces) associated with the $\mathbf{e}_i$ direction which are indexed k_i and k_i+1. The "dual" transformation associates with each open region the point

$$\mathbf{t}=\sum_{i=1}^{N} k_i \mathbf{e}_i$$

in the dual space. The set of points, $\mathbf{t}$, lies at the vertices of a complete quasicrystal packing of rhombic (or rhombohedral) unit cells with orientational symmetry corresponding to the star vectors, $\mathbf{e}_i$ (provided the $\mathbf{e}_i$ satisfy certain minor restrictions on their relative orientations; see paper II). The number of independent doublets (triplets) of star vectors (that is, ones with different sets of intersection angles) determines the maximum number of different unit cell shapes in the tiling, at most $N(N-1)/2$ in two dimensions [$N(N-1)(N-2)/3!$ in three dimensions].

In Fig. 1 we illustrate an example of a quasicrystal obtained via the GDM for an arbitrary star of seven vectors. Further discussion of the properties of GDM is given in Ref. 21 and paper II.

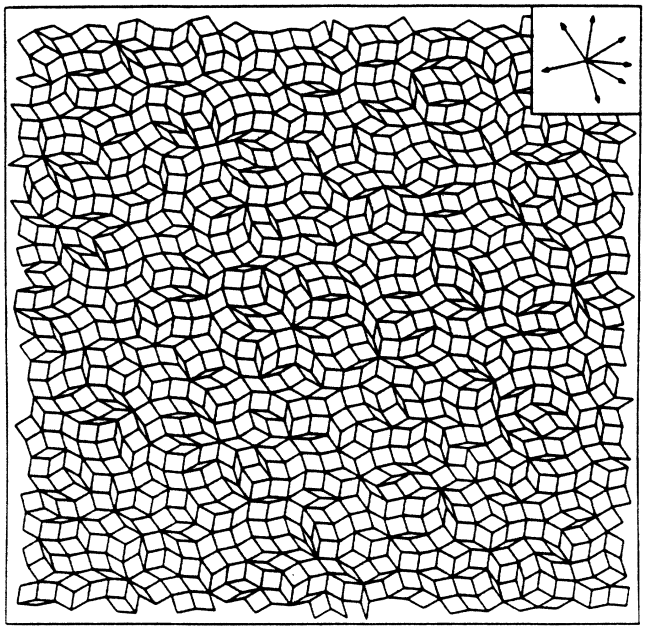

FIG. 1. A tiling generated via the GDM from a 7-grid for the set of seven arbitrary star vectors shown at the upper right.

D. A major example: Penrose tilings and the Ammann quasilattice

The inspiration for the notion of quasicrystals came from an extended study of the properties of (2D) Penrose tilings.[24,29] Penrose discovered a pair of tile shapes (in the current jargon, unit cells) plus a set of "matching rules" which determine how they are allowed to join together such that the tiles are forced to fill the 2D plane only "nonperiodically" (today we would say quasiperiodically). In Fig. 2 a small section of a Penrose tiling composed of "fat" and "skinny" rhombic unit cells is shown.

The tiling corresponds to a 2D pentagonal quasicrystal.

(a) Each edge in the Penrose tiling is oriented normal to the symmetry axis of a pentagon. Thus, a Penrose tiling has perfect pentagonal orientational order even though

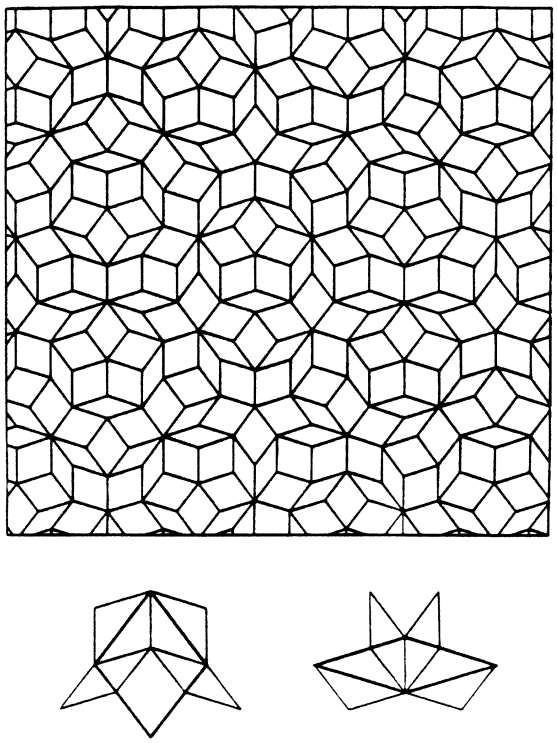

FIG. 2. Portion of a Penrose tiling with fat and skinny rhombic unit cells. The deflation rules for the two cells are shown at the bottom.

pentagonal point symmetry is disallowed for crystals in two dimensions. (Here we describe the Penrose tiling as having pentagonal orientational symmetry; however, since an edge has an orientation but not a direction, like a "headless arrow," it is equivalent to describe the tiling as exhibiting decagonal orientational symmetry.)

(b) The structure obviously has a minimal separation between vertices.

The tiling is also self-similar. The Penrose matching rules are in one-to-one correspondence with a self-similarity transformation called a *deflation rule*. The deflation rule is a decoration of the unit cells with markings which join to form a new tiling with all unit cells scaled down by a constant factor, as shown at the bottom of Fig. 2. Any cluster of tiles consistent with the matching rules can be obtained by deflating a smaller cluster of tiles.

It should be emphasized that the Penrose tilings are special in that the self-similarity transformation is so simple. As we shall discuss in paper II, many other tilings can be constructed from the same unit cells and with the same orientational symmetry. These tilings disobey the Penrose matching rules and have much more complicated self-similarity transformations.[37,38]

(c) The 2D quasiperiodic translational order is the least obvious property of the tilings. There are several ways of demonstrating the quasiperiodicity. One way is to superimpose two Penrose tilings translated by a small amount to form a moiré pattern (see Fig. 3).[39] The appearance of stripes in the moiré pattern, where the two patterns interfere constructively or destructively, directly demonstrates the translational order of the structure, although it is clearly not periodic.

The quasiperiodicity can be best observed by studying a special decoration of the Penrose tiles. Ammann[40] has pointed out that, if each tile is decorated with line segments according to Fig. 4 and then laid in a Penrose tiling according to the matching rules, the line segments join to form sets of continuous lines running parallel to each of the symmetry axes of a pentagon. According to the definitions set in Sec. II B, the continuous lines form an N-grid; furthermore, the N-grid satisfies the necessary criteria such that its intersections form a quasilattice which we will refer to as an *Ammann quasilattice*, to distinguish it from other quasilattices that can be found with the same or other orientational symmetry. The tiling can be viewed as *decoration* of the Ammann quasilattice, analogous to decorating a simple-cubic lattice to form, say, a face-centered-cubic lattice.

The position of the Nth line of any given grid from the origin is given by

$$x_N = N + \alpha + \frac{1}{\tau}\left\lfloor \frac{N}{\tau} + \beta \right\rfloor , \tag{1}$$

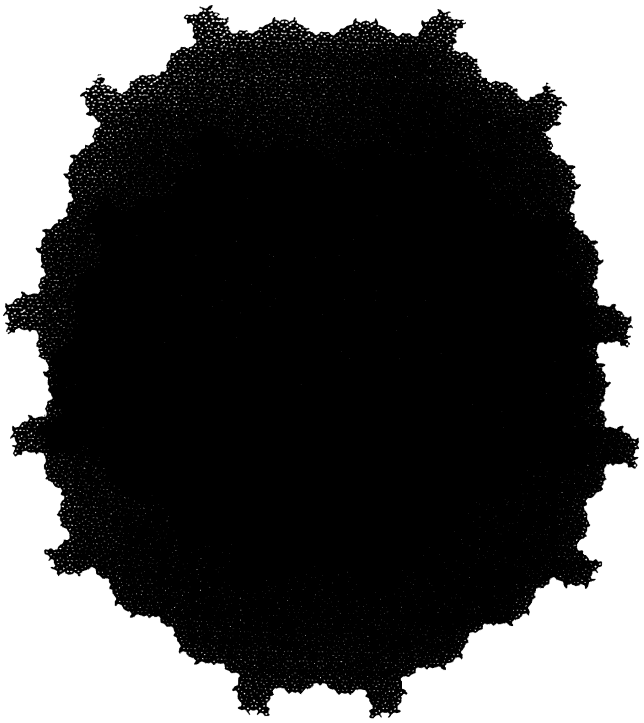

FIG. 3. Two identical Penrose tilings, one translated with respect to the other, are overlayed to form a moiré pattern. Where the two patterns interfere constructively or destructively, light or dark lines appear.

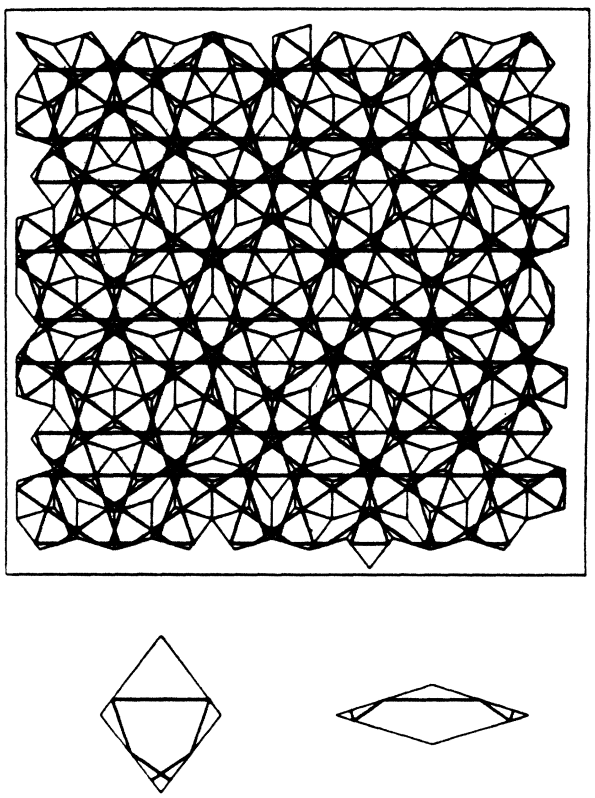

FIG. 4. Each tile in Fig. 2 has been decorated with line segments as shown at the bottom of the page. These segments join to form five sets of quasiperiodically spaced parallel lines whose locations are given by Eq. (1). The intersections of these lines comprise the Ammann quasilattice.

where τ is the golden ratio equal to $(1+\sqrt{5})/2$; α and β are arbitrary real numbers and where $\lfloor\ \rfloor$'s represent the greatest integer function. The first term alone corresponds to a periodic spacing between grid lines with spacing equal to one. The second term increases by τ^{-1} each time N is increased by τ. Because τ and 1 are relatively irrational, Eq. (1) describes a quasiperiodic spacing of lines. The spacing between any two consecutive lines $(x_N - x_{N-1})$ is L or S where $L/S = 1+1/\tau$, and the sequence of L's and S's is a Fibonacci sequence.[5] Note that Eq. (1) describes a quasiperiodic function even if τ is replaced by any irrational number. We shall see that Eq. (1) is the key to understanding the properties of the 2D Penrose tiling and the 3D icosahedral analogue.

E. 1D quasicrystals, algebraic numbers, and substitution rules

Let us consider a 1D quasicrystal with atoms placed at positions x_N, given by Eq. (1). According to the discussion above, such a structure is quasiperiodic even if τ is replaced by *any* irrational number. However, as we shall see in Sec. II F, in order to form two- and three-dimensional quasicrystals with orientational symmetry corresponding to some regular polygon in two dimensions or polyhedron in three dimensions,[36] only a special class of irrational numbers known as *algebraic numbers* can appear.[41] (Algebraic numbers are irrational numbers that satisfy a polynomial equation with integer coefficients. The degree of an algebraic number, ϕ, is defined as the degree of the lowest-order polynomial equation satisfied by ϕ. The golden ratio τ, for example, satisfies $\tau^2 - \tau - 1 = 0$ and is an algebraic number of degree two.) We shall therefore restrict our discussion of the 1D quasicrystals to cases involving algebraic numbers.

The 1D quasicrystal generated using Eq. (1) with τ being the golden ratio is self-similar. All neighbor atoms are separated by either L or S where $L/S = \tau$ [$S = 1$ in the normalization we have used in Eq. (1)]. (See Fig. 5.) Associated with the sequence of L's and S's is a "substitution" (or "production") rule: $L \rightarrow LS$ and $S \rightarrow L$, which can be expressed as

$$\begin{bmatrix} L \\ S \end{bmatrix} \rightarrow \begin{bmatrix} 1 & 1 \\ 1 & 0 \end{bmatrix} \begin{bmatrix} L \\ S \end{bmatrix} . \tag{2}$$

Under a substitution, a sequence of intervals described by Eq. (1) is transformed to another such sequence (with changes in the values of α and β in general). The action of this substitution rule on a sequence of two different elements was first studied by Leonardo Pisano (original name, Leonardo Fibonacci)[42] who showed that, beginning with a single L, say, and iterating the substitution to infinity, the ratio of l (identically equal to the number of L's) to s (identically equal to the number of S's) approaches the golden ratio τ. We therefore refer to this particular sequence of spacings as the *Fibonacci sequence.* This substitution rule for the sequence of L's and S's can be transformed into a self-similarity transformation or *inflation rule* (the inverse is a *deflation* rule) for the 1D lattice provided the ratio of lengths satisfies $L/S = \tau$, as is the case in Eq. (1): Since the ratio of interval L to the interval which is substituted for it, namely $L+S$, is equal to the ratio of S to the interval which is substituted for it, namely L, i.e.,

$$\frac{L}{L+S} = \frac{S}{L} \quad \text{or} \quad \left\lfloor \frac{L}{S} \right\rfloor^2 = \left\lfloor \frac{L}{S} \right\rfloor + 1 , \tag{3}$$

the substitution rule acting on the sequence of intervals is equivalent to a self-similarity transformation acting on the lattice points, x_N.

These properties can be generalized by considering k lengths (L_i), at least some of which must be incommensurate, and a substitution rule:

$$(L_i) \rightarrow M_{ij}(L_j) . \tag{4}$$

The matrix M_{ij} is a $k \times k$ nonsingular matrix with nonnegative integer coefficients whose eigenvalues satisfy a polynomial equation of kth degree (i.e., they are algebraic numbers). A further generalization is to consider quasicrystals obtained using a sequence of different substitution rules. This can lead to a situation where different L intervals in the sequence, say, transform differently under the deflation rules.[38] We also note that it is possible to find matrices M_{ij} that lead to structures that are not, strictly speaking, quasiperiodic (e.g., the Fourier transform may not consist of true Bragg peaks), even though they are self-similar.[36]

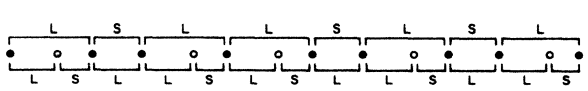

FIG. 5. 1D quasicrystal generated according to Eq. (1). The original sequence of L's and S's is shown above the lattice sites and corresponds to separations between only those sites indicated by solid disks. The deflated quasicrystal, obtained by applying the substitution rule of Eq. (2), consists of all of the sites, solid and open. The corresponding sequence of L's and S's is indicated below the sites.

F. Two- and three-dimensional quasicrystallography

The new element in extending quasiperiodic translational order from one dimension to two or three dimensions is the orientational symmetry. Just as periodicity is allowed only for special (crystallographic) orientational symmetries, so quasiperiodicity, as characterized by a set of irrational numbers, is allowed only for special orientational symmetries. Thus, there is a classification of quasicrystals that is a natural extension of the well-known classification of crystals.

A (trivial) category of quasicrystals contains structures with crystallographic orientational symmetry. As noted in the Introduction, such cases correspond to incommensurate crystals.[32] In many cases incommensurate crystals can be resolved into two or more overlapping layers of periodically spaced atoms with incommensurate periods. However, the term has been broadly defined to refer to any crystal structure with quasiperiodic modulations, a definition which incorporates the notion of quasicrystals

with crystallographic orientational symmetry. In the known physical examples, quasiperiodic structural modulation occurs only in one or two dimensions, although systems with quasiperiodic spin modulations in three dimensions are known; e.g., in chromium.[43]

For incommensurate crystals the orientational symmetry places no constraint on the quasiperiodicity—any irrational length scales (as defined by the ratio of the lengths of the wave vectors in the diffraction pattern) will do. The physical consequence is that the ratios of incommensurate lengths measured in incommensurate crystals may change continuously with temperature and pressure. The quasiperiodicity and orientational symmetry are totally decoupled.

The more interesting cases are quasicrystals with noncrystallographic orientational symmetry. In these cases, the quasiperiodic, rather than periodic, translational order allows quasicrystals with arbitrary orientational symmetry to be constructed.[19,21] At the same time, the orientational symmetry constrains the allowed incommensurate length scales and quasiperiodicity.

To demonstrate this, consider five sets of periodically spaced parallel lines oriented normal to the symmetry axes of a hexagon and a pentagon. In Fig. 6 we show a few of the lines for the hexagonal and pentagonal cases. Consider the intersections of sets 1 and 2 with set 3. For the hexagon, the spacing between intersections is the same for each set, which is directly related to the fact that a periodic lattice with hexagonal symmetry is possible. On the other hand, the spacing between intersections is different for the pentagon. In fact, the ratio of the intervals between intersection points for sets 1 and 2 with set 3 is irrational—the golden ratio τ. Thus, if the complete sets of parallel lines were drawn, intersections from set 1 would approach arbitrarily close to intersections from set 2 and the minimal separation condition would not be satisfied. This is directly related to the fact that a pentagonal periodic lattice (with minimal separation) is not possible. On the other hand, if the sets of equally spaced lines are replaced with lines with *two* fundamental spacings, L and S where $L/S=\tau$, and if the lines are spaced quasiperiodically according to the Fibonacci sequence, a lattice with minimal separation is possible. The result is the Ammann quasilattice which can be decorated with rhombuses to form a Penrose tiling.

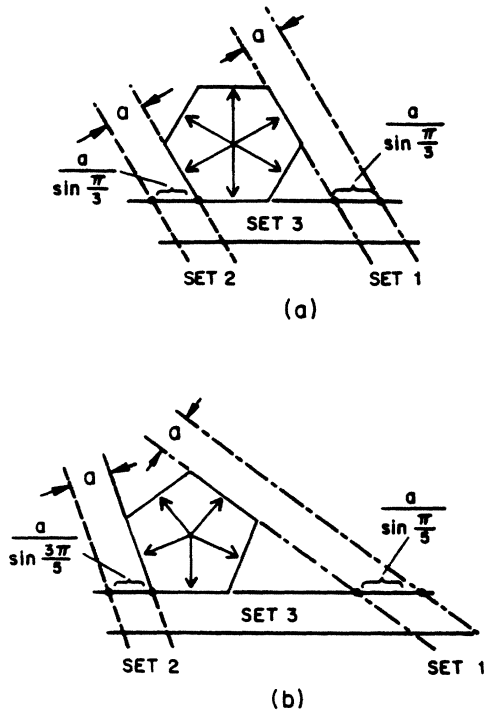

FIG. 6. Periodically spaced parallel lines with spacing a are drawn normal to the symmetry axes of (a) a hexagon and (b) a pentagon. Only a few lines from three sets are shown for each. Note that the intervals between intersections of sets 1 and 2 with set 3 are the same for the hexagon but are different for the pentagon for which ratio of interval lengths is the golden ratio.

By relaxing the constraint on the translational order from being periodic to quasiperiodic, a space-filling structure built from unit cells can be constructed with a disallowed crystallographic orientational symmetry. An important point, though, is that the irrational spacings cannot be arbitrary. The *orientational symmetry constrains the quasiperiodicity* (that is, the irrational length scales). Because intervals between intersections whose lengths are in the golden ratio are automatically generated by constructing parallel lines normal to the pentagonal symmetry axes, as shown in Fig. 6, the irrational numbers that determine the quasiperiodic spacing must contain the algebraic field[44] generated by τ in order that the minimal separation condition be satisfied. The Fibonacci sequence expressed in Eq. (1) is the simplest example. A sequence generated by $(\sqrt{2}-1)$, say, does not work for the pentagonal case because there is no minimal separation between lattice points (though it does work for the octagonal case).[45]

The following summarizes our approach to categorizing quasicrystal structures (see paper II for details). Quasicrystals can be classified according to their orientational symmetry and quasiperiodicity (that is, the irrational ratios or incommensurate length scales). Any orientational symmetry is possible. For a subset of symmetries, including those corresponding to regular polygons in two dimensions and polyhedra in three dimensions (e.g., pentagonal and icosahedral symmetry), the irrational ratios of length scales are algebraic numbers and the structures are self-similar in the general sense described in Sec. II E.

For a given symmetry and quasiperiodicity (self-similar or not), there are many local isomorphism (LI) classes; tilings with the same symmetry but in distinct classes can be constructed from the same unit-cell shapes, but some of the arrangements of cells found in each tiling are never found in the other. For a given symmetry and quasiperiodicity, the GDM produces an infinite range of LI classes.

We shall argue in Sec. IV that only configurations in the same LI class have the identical diffraction patterns and free energies. Thus, discrimination between LI classes is physically significant; for example, it is impor-

tant to realize that only locally isomorphic tilings are energetically equivalent when counting the degeneracy of the ground state.

A special LI class that we will call the *Penrose local isomorphism* (PLI) *class* (because the original Penrose tiling corresponds to this class for the pentagonal case) has three very special properties: (a) there exist matching rules for the unit cells such that any tiling which fills space is forced to be a quasicrystal in the class; (b) there exists a simple self-similarity transformation or deflation rule (as shown in Fig. 2 for the Penrose tiles); (c) there exists a decoration of the unit cells with line segments or planar sections such that the segments or sections join to form a quasilattice (analogous to the Ammann quasilattice shown in Fig. 4) when the cells are packed into a tiling. We shall see in paper II that the three properties are closely related. This class might be especially interesting if the matching rules can be enforced by local interactions of atoms or clusters. In this case, the ground state of the atomic system might be a structure that is an element of the Penrose class.

G. Structure of icosahedral quasicrystals

The icosahedral quasicrystal is a case of special interest: the one which is relevant to the earlier work on icosahedral ordering in supercooled liquids and glass (see comments in Sec. VI); and the one which appears to describe the recently observed Al-Mn alloy.[6,5]

The simplest set of unit cell shapes for the icosahedral quasicrystal consists of the oblate and prolate rhombohedra shown in Fig. 7. (These play similar roles to the skinny and fat tiles, respectively, in the 2D Penrose tiling.) All the faces are identical rhombuses. As first described by Kowalewski,[46] ten prolate and oblate rhombohedra can be packed to form a rhombic triacontahedron, a zonohedron with icosahedral symmetry. A general 3D icosahedral quasicrystal packing of the unit cells consists of a ratio of prolate to oblate rhombohedra equal to τ:1. Figure 8(b) shows a layer of such a rhombohedral packing.

A case of special interest is the packing corresponding to the PLI class—the 3D icosahedral analogue of the 2D Penrose tiling. This class is defined by a set of unit-cell shapes plus rules for matching them face on face such that the rhombohedra can only fill space quasiperiodically. The set of matching rules is in one-to-one correspondence with a deflation algorithm. That is, the constraints on the way two cells can match face to face imposed by the matching rules are identical to constraints required for unit-cell packing to be deflatable; alternatively, any finite packing of unit cells in accordance with the matching rules can be inflated and deflated, and, if a packing is built according to the matching rules and then deflated or inflated, the new packing again obeys the matching rules. Independently of our own construction,[5,47] several groups have attempted to obtain such a packing. Ammann attempted a construction using the same rhombohedral unit cell shapes,[40] as reported by Mackay;[48] Kramer[49] and, independently, Mosseri and Sadoc[50] have suggested different sets of shapes (each set containing more than two unit cells). However, the matching rules provided were either incomplete, the construction required a center of symmetry, and/or the unit cells were not forced to match vertex to vertex (which can result in there being effectively an infinite number of matching rules). Mackay and Mosseri and Sadoc also suggested that the icosahedral structure might have some relevance to atomic structures, although they never identified the full symmetries, particularly the quasiperiodicity, of such a structure.

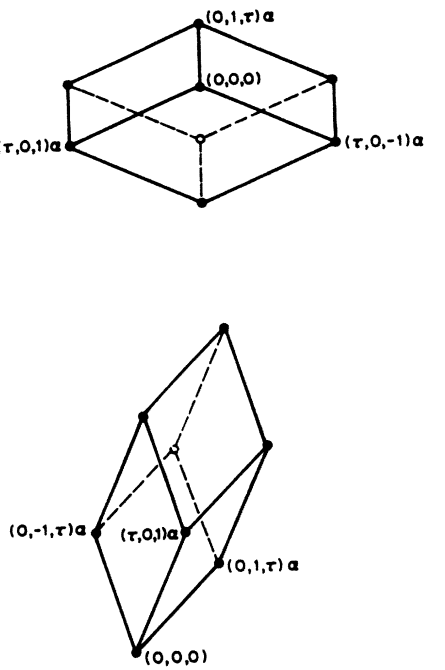

FIG. 7. The two rhombohedral unit cells used to build the icosahedral quasicrystal packing. The ratio of volumes of the prolate rhombohedron (lower) to the oblate one is τ. If $a=(1+\tau^2)^{1/2}$, the edge lengths are unity.

As for our own construction, we found that the matching and deflation rules as applied to the rhombohedra are much more complicated than the 2D analogue.[5,47] Two rhombohedra with the same shape may have different matching and deflation rules, or rules for a given unit cell may depend upon the local packing configuration about that cell. An alternative and much more useful construction makes use of four types of unit cells, each of which is a zonohedron that can be formed from the oblate and prolate rhombohedral bricks: (a) a rhombic triacontahedron formed from ten oblate and ten prolate bricks; (b) a rhombic icosahedron formed from five oblate and five prolate bricks; (c) a rhombic dodecahedron formed from two oblate and two prolate bricks; and (d) a single prolate rhombohedron. Associated with these four units is a set of planes whose intersections are the 3D analogue of the Ammann quasilattice of the 2D Penrose tiling. Wherever a zonohedron of a given shape is found in the structure it is divided by the planes in the same way. If the four zonohedra are used as the fundamental bricks for the icosahedral quasicrystal instead of the rhombohedra, the matching rules reduce to the constraint that bricks only be matched in such a way that all the planes are continuous-

ly extended across the interface. Also, using the GDM, the deflation rules may be determined from the intersections of the planes. Thus, two zonohedra with the same shape have the same matching and deflation rules. In Fig. 8 we show a layer of the zonohedral packing and, below it, the decomposition of the layer into the two rhombohedra unit cells (the decomposition actually includes some additional rhombohedra above and below the depicted layer which have been removed for the sake of clarity). The detailed construction of the PLI class packing is given in paper II.

Of course, as pointed out in Sec. II F, this matching rule construction produces only a single local isomorphism (LI) class of icosahedral packings, albeit a very interesting one. The icosahedral packings generated by projections from a six-dimensional hypercubic lattice also are elements of a single (different) class; the GDM produces elements of infinitely many other classes. However, these other classes do not have simple deflation and matching rules.

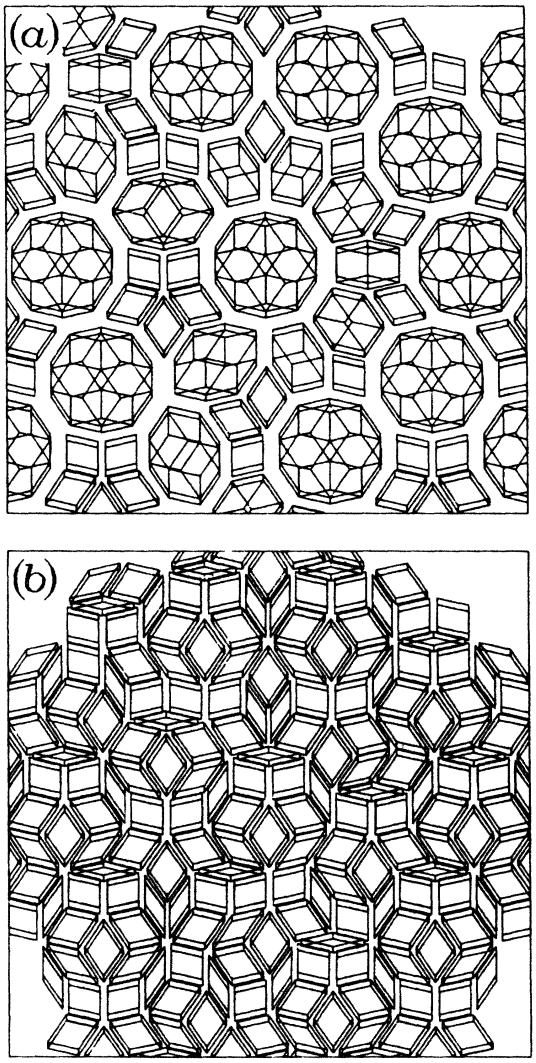

FIG. 8. Layer of a 3D icosahedral quasicrystal packing corresponding to the Penrose local isomorphism (PLI) class. In (a), the layer is shown as a packing of the four zonohedral unit cells. The unit cells can be decomposed into the rhombohedral unit cells of Fig. 7, as shown in (b) (the decomposition actually includes some additional rhombohedra above and below the depicted layer which have been removed for the sake of clarity).

A complementary approach to describing quasicrystals is from the point of view of Landau theory.[12,15,16,18,17,51] Just as for crystals, there exists a Landau theory and density wave description for the quasicrystal structure. Associated with the star of N vectors that define the orientational symmetry are a set of N fundamental density waves, ρ_i. The ρ_i are the leading Fourier coefficients in the transform of the density function for the quasicrystal. A Landau free-energy expression can be written as an expansion in the ρ_i. In a density wave approximation, only the leading terms are kept and the structure is approximated as a sum of the fundamental density waves.

The quasicrystal model and the density wave description bear the same relation to one another as the crystal lattice and density wave picture for crystals. Both pictures are useful for describing various properties. No direct information about atomic structure is provided by the density wave description; in fact, the density wave description is not usually useful for describing the microscopic structure of solids that are not near the melting temperature. Better approximations to microscopic structure can be obtained in principle by keeping more and more terms in the Fourier transform of the density. However, a more useful microscopic description of a quasicrystal solid is in terms of the atomic decorations of the unit cells. On the other hand, the Landau description is useful for studying the hydrodynamics and elasticity theory.[16,52,53]

H. Diffraction patterns

The diffraction pattern of a quasicrystal is one of its most distinctive features. The pattern consists of a set of Bragg peaks that densely fill reciprocal space. This result can be understood intuitively by considering the case of the one-dimensional quasicrystal with atomic positions given by Eq. (1). As described in Sec. II D, Eq. (1) can be divided into a sum of two functions that describe periodic spacings but with incommensurate periods. If the first term only were kept, the diffraction pattern would consist of Bragg peaks spaced periodically in reciprocal space with some fundamental period k_0. Because the second term is incommensurate, it leads to Bragg peaks at some incommensurate reciprocal space period k_1. The full pattern then consists of the union of the two sets of peaks, plus peaks at linear combinations of k_0 and k_1. Because the two are incommensurate, the peaks densely fill reciprocal space (in a countable, nonfractal way). For a two- or three-dimensional quasicrystal, the reciprocal space is still densely filled with Bragg peaks, but now in a 2D or 3D pattern whose rotational symmetry reflects the orientational order. The position of each peak in the pattern can be written as an integral linear combination of the N reciprocal-lattice vectors associated with the star of N vectors. In Sec. III we discuss the quantitative computation of the intensities of the diffraction pattern.

The fact that the diffraction pattern consists of a dense set of Bragg peaks has physical implications for the spectrum of electron and phonon states. In the nearly-free-electron approximation, the gaps in the energy spectrum are in one-to-one correspondence with the Bragg peaks and the gap sizes scale with the intensities; thus, the spectra are expected to consist of a set of gaps that are dense in k space.[5] Since the intensities of peaks very near a peak of given intensity are much less intense in general, near a large gap there are arbitrarily weak ones; therefore, we do not expect the dense set of gaps to drastically alter the behavior of quasicrystals compared to crystals, although more accurate computations are needed.

III. DIFFRACTION PATTERN OF ICOSAHEDRAL QUASICRYSTALS

The diffraction pattern of the icosahedral quasicrystal consists of a set of Bragg peaks that densely fill reciprocal space in an array with icosahedral symmetry. To explain this result, we will first consider the case of a one-dimensional quasicrystal with atomic positions given by Eq. (1). This particular example is critical in the study of the pentagonal and icosahedral quasilattices.

A. Diffraction pattern for a 1D quasicrystal

The atomic positions of the 1D (Fibonacci) quasicrystal described by Eq. (1) may be reexpressed as

$$x_n = n\left[1+\frac{1}{\tau^2}\right]+\beta\sqrt{5} + \left[-\frac{1}{\tau}\left\{\frac{n(1+1/\tau^2)+\beta\sqrt{5}}{\sqrt{5}}\right\}-\beta\tau+\alpha\right], \quad (5)$$

where the curly brackets signify the fractional part (or mod1) function and we have used the fact that $\tau(1+1/\tau^2)=\sqrt{5}$. (An identity is $x=\lfloor x\rfloor+\{x\}$. The function $\{x\}$ is periodic in x with period 1.) This expression is of the general form:

$$x_n = na+\phi+F(na+\phi), \quad (6)$$

where $F(x)$ is periodic in x with period b and a/b is irrational. Expressions of this variety arise in the study of the Frenkel-Kontorova model,[32] which describes a 1D incommensurate crystal. The Fourier transform of such a set of atomic positions consists of Bragg peaks at positions $k=2\pi M/a+2\pi N/b$, where M and N are integers. For our case, this means that there will be peaks at

$$k_{pq}\equiv\frac{2\pi}{1+1/\tau^2}\left[p+\frac{q}{\tau}\right], \quad (7)$$

where p and q are integers.

In order to see this result explicitly, we will employ an argument based on the fact that numbers of this form constitute a dense subset of the real numbers (that is, arbitrarily close to any real number is a number of this form). We will compute the diffraction pattern (i.e., Fourier transform) of the 1D quasicrystal in Eq. (1):

$$f_1(k)=\lim_{N\to\infty}\left[\frac{1}{N}\sum_n \exp(ikx_n)\right], \quad (8)$$

where we are summing over the N atomic position in a 1D chain. First, consider $f_1(k)$ for k of the form, $k=k_{pq}$, as defined in Eq. (7); noting the identity $\tau(1+1/\tau^2)=\sqrt{5}$, the exponent in Eq. (8) is given by

$$\begin{aligned} ik_{pq}x_n &= 2\pi i\left[pn+q\frac{n}{\tau}\right]+k_{pq}\left[\frac{\beta}{\tau}+\alpha-\frac{1}{\tau}\left\{\frac{n}{\tau}+\beta\right\}\right] \\ &= 2\pi i\left[pn+q\left[\frac{n}{\tau}+\beta\right]\right]+i\left[2\pi q-\frac{k_{pq}}{\tau}\right]\left\{\frac{n}{\tau}+\beta\right\} \\ &\quad +ik_{pq}\alpha-i\left[2\pi q-\frac{k_{pq}}{\tau}\right]\beta, \end{aligned} \quad (9)$$

where we have used the identity $x=\lfloor x\rfloor+\{x\}$ to obtain the second expression. The first term in the final expression is an integer times $2\pi i$, and therefore only contributes a factor of unity upon exponentiation. The last two terms are independent of n, and so only contribute an overall phase factor to $f_1(k)$. The second term, however, is n dependent and contributes to the sum in an important fashion. Since

$$0\le\left\{\frac{n}{\tau}+\beta\right\}\le 1,$$

the second term lies between zero and iX, where

$$X\equiv 2\pi q-\frac{k_{pq}}{\tau}. \quad (10)$$

Since τ is an irrational number, the value of the second term is *uniformly and densely* distributed in the interval $(0,X)$, enabling us to approximate the sum in Eq. (8) by an integral:

$$f_1(k)=\frac{e^{i\psi}}{X}\int_0^X \exp(iy)dy=\frac{\sin(X/2)}{X/2}\exp(i\gamma), \quad (11)$$

where

$$\psi\equiv k_{pq}\alpha-\left[2\pi q-\frac{k_{pq}}{\tau}\right]\beta \text{ and } \gamma\equiv\psi+\frac{X}{2}. \quad (12)$$

Equation (11) is the value of $f_1(k)$ for the special values of $k=k_{pq}$, which, we argued in Eqs. (5) and (6), correspond to the positions of Bragg peaks. To make this more plausible, consider any point k' that is not of the form k_{pq}. Then k' can be arbitrarily well approximated by an expression of the form k_{pq}, because these points densely fill reciprocal space. There exists a well-defined, uniform sequence of best approximants to k' of the form k_{pq}.[41,42] However, the integer q becomes arbitrarily large with improving approximation while the value of k_{pq} remains nearly unchanged. Thus, X in Eq. (10) also grows arbitrarily large and the amplitude of $f_1(k)$, according to Eq. (11), approaches zero. From this we conclude that

$$f_1(k)=\sum_{pq}\left[\frac{\sin(X/2)}{X/2}e^{i\gamma}\right]\delta(k-k_{pq}). \quad (13)$$

Those familiar with the computation of the Fourier transform of the 1D quasicrystal via projection methods[11,54] (which appeared subsequent to Ref. 5) will recognize that the two methods agree exactly.

The brightest spots occur for those $k=k_{pq}$ where X is small. Since

$$X=\left|2\pi q-\frac{k_{pq}}{\tau}\right|=\frac{2\pi i}{\sqrt{5}}(q\tau-p), \tag{14}$$

this means that q/p must be close to τ. It is well known that the best rational approximants to τ occur when q and p are successive Fibonacci integers, F_n.[42] Therefore, the sequence of most intense peaks corresponds to $(p,q)=(F_{n+1},F_n)$, where $(F_1,F_0)=(1,1)$.

Note that the diffraction peaks are indexed by two integers even though the structure is one dimensional. The appearance of more indices than the dimensionality is typical of incommensurate crystals and quasicrystals. Since all pairs of integers are represented in general, the peaks of the diffraction pattern of the 1D quasicrystal are in one-to-one correspondence with the diffraction peaks of a two-dimensional square periodic lattice. This is directly connected with the fact that the real-space structure itself can be obtained as a projection from a two-dimensional periodic lattice.[11,54,38]

B. 3D diffraction patterns

The diffraction pattern of the 3D quasicrystal is simply related to the Fourier transform of the 1D quasicrystal, just as the 3D crystal diffraction pattern is simply expressed in terms of the transform of a 1D crystal. In Ref. 5, we presented the diffraction pattern for the quasilattice underlying the icosahedral packing. This pattern has the quasiperiodicity and orientational symmetry of the packing itself since the unit cells can be viewed as a decoration of the quasilattice. Also, the diffraction pattern of the quasilattice should have Bragg peaks in the same places as the icosahedral packing except for possible extinctions (as found in going from simple cubic, say, to fcc crystal lattices). Thus, the diffraction pattern of the quasilattice embodies all of the essential features of the diffraction pattern for the packing.

The quasilattice for a three-dimensional tiling is composed from sets of quasiperiodically spaced parallel planes. There are five models with icosahedral orientational order.[18,55] To discuss the different models, it is useful to consider the action of the full icosahedral group (including reflections) on a point P on the surface of an icosahedron. If we act on P with all the elements Y_j of the icosahedral group, we obtain the orbit of P: the set of points Y_jP. The points Y_jP divide into pairs such that each pair lies on an axis through the center of the icosahedron. We shall say that this set of axes is generated by the point P. The number of axes depends upon the symmetry of the icosahedron about the point P.

The five quasilattice models with icosahedral orientational symmetry are described as follows:

(1) Sets of planes oriented normal to the *six* axes generated by a point of fivefold symmetry of the icosahedron (a vertex).

(2) Sets of planes normal to the *ten* axes generated by a point of threefold symmetry (a face center).

(3) Sets of planes normal to the *fifteen* axes generated by a point of (2×2)-fold symmetry (an edge center).

(4) Sets of planes normal to the *thirty* axes generated by a point of reflection symmetry (that is not one of the points of higher symmetry discussed in the models above).

(5) Sets of planes normal to the *sixty* axes generated by a point P that is not a symmetry point of the icosahedron.

In the nomenclature of Ref. 21, the first model is called the vertex model, the second is called the face model, and the third is called the edge model. Although the diffraction patterns for all the models possess icosahedral symmetry, there will be differences both in the locations and intensities of the diffraction spots, particularly in the planes normal to the (2×2)-fold symmetry axes.[18,56] The original experiments of Shechtman *et al.*[6] appear to correspond to the vertex model. There is also the suggestion that the T phase of Al-Mn is really a structure described by periodic stacking of decagonal quasicrystals,[31,51] roughly analogous to a hexagonal prism structure, a possibility mentioned in Ref. 21.

Neither the quasilattices nor the three-dimensional tilings associated with them constitute a realistic atomic model for I-Al-Mn or similar alloys. A packing of Al and Mn in the unit cells is required. Aluminum and manganese scatter differently, whereas the theoretical models above use ideal point atoms of a single type. Many decorations are possible, including ones where two unit cells of the same shape are decorated differently. The tiling associated with the quasilattice represents the analogue of a Bravais lattice. From the diffraction patterns of the quasilattices or tilings one can learn the qualitative features about the diffraction pattern of I-Al-Mn, such as the symmetry and the location of the Bragg peaks (except for possible extinctions), but it is probably not useful to directly compare the computed intensities to the experimental data.

The diffraction pattern of the quasilattices for the various models can be computed straightforwardly. We shall introduce the same formalism for all the models and then discuss the vertex model in detail as an example.

The vertices $\mathbf{x}$ of a quasilattice lie at the intersections of three planes, and so satisfy three simultaneous equations:

$$\begin{aligned}&\mathbf{e}_i\cdot\mathbf{x}=x_n,\\&\mathbf{e}_j\cdot\mathbf{x}=x_{n'},\\&\mathbf{e}_k\cdot\mathbf{x}=x_{n''},\end{aligned} \tag{15}$$

where $i\neq j\neq k$; $\mathbf{e}_i$ is the unit normal to the ith family of planes; and x_n is given by Eq. (1). (In general, α and β may be different for different sets of planes.) We may write Eq. (15) as a matrix equation:

$$\mathbf{M}_{ijk}\mathbf{x}=\mathbf{v}, \tag{16}$$

where

$$\mathbf{M}_{ijk}=\begin{bmatrix}\mathbf{e}_i\\\mathbf{e}_j\\\mathbf{e}_k\end{bmatrix}\quad\text{and}\quad\mathbf{v}=\begin{bmatrix}x_n\\x_{n'}\\x_{n''}\end{bmatrix}. \tag{17}$$

Here i, j, and k vary from 0 to 5 for the vertex model, 0 to 9 for the face model, and 0 to 14 for the edge model. Equation (16) can be inverted to obtain $\mathbf{x}$, which is what is needed to compute the Fourier transform of the quasilattice:

$$F_3(\mathbf{k}) = \sum_{i>j>k} \sum_{n,n',n''} \exp(i\mathbf{k}\cdot\mathbf{x}) . \tag{18}$$

For a given i, j, and k, the exponent can be expressed:

$$i\mathbf{k}\cdot\mathbf{x} = i\mathbf{k}\cdot(\mathbf{M}_{ijk}^{-1}\mathbf{v})$$
$$= i(\mathbf{k}\cdot\mathbf{u}_{ijk}x_n + \mathbf{k}\cdot\mathbf{u}_{jki}x_{n'} + \mathbf{k}\cdot\mathbf{u}_{kij}x_{n''}) , \tag{19}$$

where

$$\mathbf{u}_{ijk} \equiv \mathbf{e}_j \times \mathbf{e}_k / [(\mathbf{e}_i \cdot (\mathbf{e}_j \times \mathbf{e}_k)]$$

and

$$\mathbf{M}_{ijk}^{-1} = (\mathbf{u}_{ijk}\, \mathbf{u}_{jki}\, \mathbf{u}_{kij}) .$$

Thus, the 3D Fourier transform of the quasilattice breaks up into a product of 1D transforms and can be written

$$F_3(\mathbf{k}) = \sum_{i>j>k} f_1(\mathbf{k}\cdot\mathbf{u}_{ijk}) f_1(\mathbf{k}\cdot\mathbf{u}_{jki}) f_1(\mathbf{k}\cdot\mathbf{u}_{kij}) . \tag{20}$$

Since we have shown that the support of $f_1(k)$ (i.e., the set of k where the function is nonzero) is the set $k = k_{pq}$ (see Sec. III A), the argument of each factor in Eq. (20) must be of this form in order that $F_3(\mathbf{k})$ not vanish. This occurs for $\mathbf{k}$ of the form:

$$\mathbf{k} = \frac{2\pi}{\sqrt{5}} \left[\left[p_i + \frac{q_i}{\tau} \right] \mathbf{e}_i + \left[p_j + \frac{q_j}{\tau} \right] \mathbf{e}_j + \left[p_k + \frac{q_k}{\tau} \right] \mathbf{e}_k \right] , \tag{21}$$

where $\mathbf{e}_i, \mathbf{e}_j, \mathbf{e}_k$ $(i \neq j \neq k)$ are three of the N star vectors and where the p_i and q_i are integers. (We use the same vectors $\mathbf{e}_i$ to denote both the real-space and reciprocal-space basis vectors.)

The unit normals, $\mathbf{e}_i$ are as follows.

(a) Vertex model: $[1/(1+\tau^2)^{1/2}](0, \tau, \pm 1)$, plus cyclic permutations.

(b) Face model: $(1/\sqrt{3})(0, \pm\tau^{-1}, \tau)$ and $(1/\sqrt{3})(-1,1,1)$ plus cyclic permutations of each, and $(1/\sqrt{3})(1,1,1)$.

(c) Edge model: (1,0,0) plus cyclic permutations, and $\frac{1}{2}(\pm\tau, \pm\tau^{-1}, 1)$ plus cyclic permutations.

An electron diffraction pattern corresponds to a set of spots that lie in some plane that passes through the origin of reciprocal space. For the choice of coordinates we have used above, the z axis corresponds to a (2×2)-fold symmetry axis. Thus, examples of planes normal to the (2×2)-fold, fivefold, and threefold symmetry axes correspond to $k_z = 0$, $k_x + \tau k_z = 0$, and $\tau^2 k_x + k_z = 0$, respectively.

C. The icosahedral (vertex) model

As a specific example, let us consider the case of the vertex model. The diffraction pattern is characterized by six indices [the six integers (p_i, q_i) in Eq. (21)], and so diffraction peaks are in one-to-one correspondence with a six-dimensional periodic hypercubic lattice. (This corresponds with the fact that an icosahedral quasicrystal rhombohedral packing can be obtained as a projection of a six-dimensional periodic hypercubic lattice down to 3D.[10–13]

Our computation of the diffraction pattern for the *quasilattice* is shown in Fig. 9; that is, this figure shows the diffraction pattern for an ideal model in which identical atoms are placed at each point of the quasilattice. Although this does not represent a realistic atomic model, the diffraction pattern is still useful for determining the positions and relative intensities of peaks for a realistic atomic decoration of the quasilattice; e.g., as might occur in I-Al-Mn. The right-hand side of the figure shows the diffraction patterns for the rapidly quenched alloy of Al and Mn observed by Shechtman *et al.*[6] The agreement with observations is remarkable; every diffraction spot observed experimentally appears in our computation. For the fivefold and threefold symmetry axes the agreement is

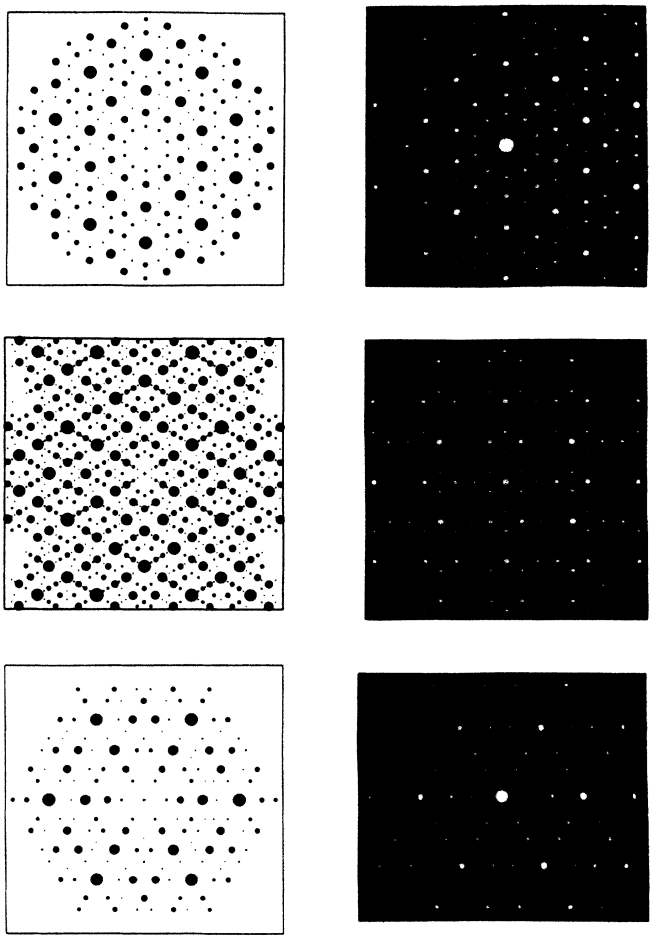

FIG. 9. Computed diffraction patterns of the icosahedral Ammann plane quasilattice (left) and the experimental electron diffraction patterns taken on a rapidly cooled alloy of aluminum manganese. (a) In a plane normal to a fivefold axis of an icosahedron. (b) In a plane normal to a threefold axis. (c) In a plane normal to a (2×2)-fold axis.

perfect. For the (2×2)-fold pattern, there are many extra spots in the quasilattice diffraction pattern that do not appear (that is, they are extinct) for *I*-Al-Mn. This result demonstrates that the diffraction pattern in the plane normal to (2×2)-fold axis is the most sensitive to the detailed decoration of the lattice.[56] By decorating the quasilattice (similar to going from fcc to bcc lattices), the unwanted quasilattice spots can be extinguished.

As it turns out, the simplest decoration that extinguishes the unwanted spots is to put identical atoms at the vertices of the rhombohedral packing that decorates the quasilattice. As with the quasilattice, this decoration is not a realistic atomic model either because there are many large vacances and there is only one atomic species. The model certainly does not apply to *I*-Al-Mn which has two atomic species. On the other hand, the initial goal is to understand the qualitative, not quantitative, features of the spectrum.

The fact that the diffraction patterns of the quasilattice and the rhombohedral packing are different is easy to understand. Consider the vertices of the packing in which each vertex lies at the intersection of several oblate and/or prolate rhombohedra. The position of each vertex can be written as an integral linear combination of the six icosahedral star vectors, $\mathbf{e}_i$. By contrast, the vertices of the quasilattice and the Bragg peaks of the quasilattice diffraction pattern correspond to integer linear combinations of the form in Eq. (21); that is, combinations of both $\mathbf{e}_i$'s and $\tau\mathbf{e}_i$'s. For the icosahedral vectors, $\tau\mathbf{e}_i$ cannot be written as an integral linear combination of the $\mathbf{e}_i$'s. Unlike the case of the packing diffraction pattern, the quasilattice pattern is defined not just by a single ring of basis vectors (the $\mathbf{e}_i$'s) but by two rings (the $\tau\mathbf{e}_i$'s as well). In the end, though, one structure is just a decoration of the other.

It is interesting to note that the extinction of the unwanted spots can also be obtained by a simple modification of the quasilattice; for example, consider a spacing of grid lines given by

$$x_n = n + \frac{2}{\tau}\left[\frac{n}{2\tau} + \beta\right] + \alpha \,. \tag{22}$$

Each point of the quasilattice is a linear combination of vectors of the form $(m + n/\tau)\mathbf{e}_i$, where n is even only [for the quasilattice generated by Eq. (1), n odd and even occurs]. Any such point of this more restricted kind *can* be written as an integral linear transform of the $\mathbf{e}_i$'s alone. The diffraction patterns of the modified quasilattice and the packing will have Bragg peaks at precisely the same points and extinctions at precisely the same points. The intensities of the two patterns will differ, but since neither corresponds to a realistic atomic model there is no need to be very concerned about such quantitative differences.

In Fig 10 we show a picture of the diffraction pattern for this modified quasilattice, which it can be seen, incorporates the correct extinctions. The two diffraction patterns exhibited in Figs. 9 and 10 illustrate another possible variation among quasicrystals with icosahedral symmetry. Along with the face, edge, etc. models discussed earlier, these correspond to different structures with the same orientational symmetry, and phase transitions between these different structures might be observed in physical systems.

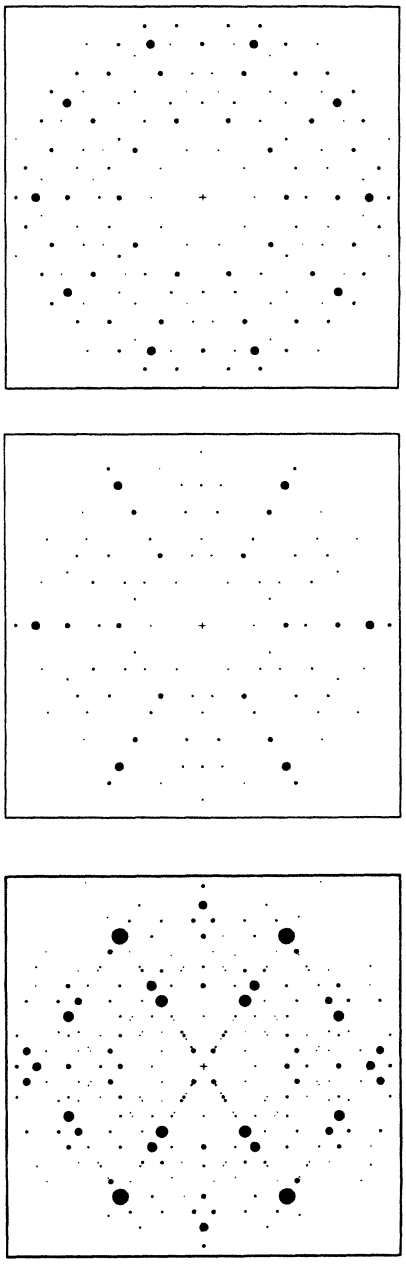

FIG. 10. Computed diffraction pattern of the modified quasilattice in the planes normal to the fivefold, threefold, and (2×2)-fold axes of an icosahedron. As can be seen, peaks in the (2×2)-fold pattern of the Ammann quasilattice (Fig. 9) have been extinguished. (In addition, there are a few new peaks in the figure compared to Fig. 9, but these are just an artifact of using a different intensity cutoff.)

The brightest peaks in either diffraction pattern correspond to those wave vectors $\mathbf{k}$ of the form shown in Eq. (21) where the coefficients, $p_i + q_i/\tau$, are such that the

$$X_i = \left| 2\pi q_i - \frac{k_{p_i q_i}}{\tau} \right| = \frac{2\pi i}{\sqrt{5}}(q_i\tau - p_i) \tag{23}$$

are as close to zero as possible. In such cases, the arguments of the factors of $f_1(k)$ in Eq. (20) are near zero and, as argued in Sec. III A [see Eq. (14)], this means $f_1(k)$ is large. The brightest peak of all, then corresponds to all $(p_i,q_i)=(0,0)$—the central peak of the diffraction pattern. The next brightest peaks occur for the case where (p_i,q_i) are nonzero for some single value of i, but $(p_j,q_j)=(0,0)$ for *two* distinct values of j not equal to i. These correspond to wave vectors oriented along one of the icosahedral basis vectors, $\mathbf{e}_i$. Among this subset of wave vectors, the intensities are ordered according to how close X_i is to zero or, equivalently, how close q_i/p_i is to τ; as was concluded in the discussion of Eq. (14), the sequence of brightest spots occurs for $(p_i,q_i)=(F_{n+1},F_n)$, or

$$\mathbf{k}=(F_{n+1}+F_n/\tau)\mathbf{e}_i\,, \tag{24}$$

where F_n represents the nth Fibonacci number. The peaks in the sequence become brighter as n increases. (This result is the same for the original and modified quasilattices except for the restriction that $q_i=F_n$ be even in the latter case.)

IV. LOCAL ISOMORPHISM

An important difference between periodic crystals and quasicrystals is that for crystals there is a unique ideal unit-cell packing (up to translations and rotations), whereas for quasicrystals there are an infinite number of distinct ideal unit-cell packings. For a periodic crystal there is a single unit cell and there is only one way to pack the cell (up to translations and rotations) so as to form an undefected crystal structure. For quasicrystals, there are two or more unit cells and many distinct quasicrystal packings which can be subdivided into different equivalence classes that we call *local isomorphism* or LI classes. Two quasicrystals in the same LI class are said to be locally isomorphic.

Two quasilattices (packings) are locally isomorphic if and only if every finite configuration of vertices (tiles) that appears in each quasilattice (packing) appears in the other. That is, two locally isomorphic quasilattices (packings) can be made to overlap out to any finite distance by a finite translation (plus global rotations and inversions) and overlap out to arbitrarily large distances if we allow arbitrarily large translations. This is sufficient to guarantee that clusters occur with equal frequency out to arbitrarily large distances. A quasilattice in one LI class will have configurations of vertices that do not appear in a quasilattice in a different LI class; a packing in one LI class will have configurations or clusters of tiles that do not appear in a packing in a different LI class.

Local isomorphism has physical significance. In particular, two quasilattices (or packings) have identical diffraction patterns if and only if they are locally isomorphic. Two quasilattices (or packings) in distinct LI classes have diffraction patterns with Bragg peaks in the same locations, but the peak intensities differ. Intuitively, one expects two locally isomorphic quasicrystals to have the same diffraction pattern because they are locally equivalent. Any finite bounded region which occurs in one also occurs in the other. Thus, no local measurement can distinguish the two structures. We will demonstrate this result for the case of the icosahedral (vertex) quasilattices described by Eq. (15).

A. Local isomorphism and diffraction patterns

Consider the quasilattices described by Eq. (15) for the case of the vertex model. In this case, each vertex lies at the intersection of three planes each of which belongs to a set of grid planes normal to one of the six basis vectors, $\mathbf{e}_i$. We will label the vectors $i=0,1,\ldots,5$ where $\mathbf{e}_5=(0,0,1)$ and

$$\mathbf{e}_n=(\sin(\eta)\cos(2\pi n/5),\sin(\eta)\sin(2\pi n/5),\cos(\eta))\,,$$

where $\cos(\eta)=1/\sqrt{5}$. The spacing of the planes for each of the six grids is identical except for the choice of α and β. We can completely specify the the ith grid by the ordered pair (α_i,β_i).

From Eqs. (11) and (12), it can be seen that changing (α,β) for the 1D quasilattice only changes ψ, which in turn only changes the relative phases of the Bragg peaks; the intensities ($\propto |f_1(k)|^2$) of the peaks are unchanged.

In two or three dimensions, though, changing (α_i,β_i) can change the relative intensities. The factors of $f_1(k)$ in each term of Eq. (20) have as their argument an expression of the form $\mathbf{k}\cdot\mathbf{u}_{ijk}$ corresponding to the contribution of quasilattice points that lie in planes that belong to the grid normal to $\mathbf{e}_i$; thus, each factor of $f_1(k)$ also depends on the (α_i,β_i) associated with that grid. In particular, each factor of $f_1(\mathbf{k}\cdot\mathbf{u}_{ijk})$ contains an α- and β-dependent phase factor, $\exp(i\psi_i)$, where

$$\psi_i \equiv k_{p_i q_i}\alpha_i - \left| 2\pi q_i - \frac{k_{p_i q_i}}{\tau} \right| \beta_i\,, \tag{25}$$

where p_i and q_i are integers. We have implicitly used the fact that, since $F_3(\mathbf{k})$ is a sum of products of $f_1(k)$, the Bragg peaks occur only when $f_1(k)$ is nonzero for each factor in at least one term of Eq. (20); or according to Sec. III A when $\mathbf{k}$ is of the form

$$\mathbf{k}\cdot\mathbf{u}_{ijk}=k_{p_i q_i}=2\pi\left[p_i+\frac{q_i}{\tau}\right]\Big/\left[1+\frac{1}{\tau^2}\right]$$

plus cyclic permutations of ijk, for some triplet of $i\neq j\neq k$. Thus, each term in Eq. (20) has a phase factor, $\exp[i(\psi_i+\psi_j+\psi_k)]$. A change in (α_i,β_i) can change the relative phase factors of the different terms in Eq. (20), thereby changing the magnitude of their sum. The result is a change in the peak intensity. (In general, the change in intensities changes the quantitative but not the qualitative features of the diffraction pattern.)

There are some shifts in the (α_i,β_i), though, that leave the Bragg peak intensities unchanged. These changes correspond either to translations of the quasilattice, or to shifts from one quasilattice to another in the same LI class. We shall briefly present the argument in the remainder of this section.

The shifts that leave the intensities unchanged are of the form $(\alpha_i,\beta_i)\rightarrow(\alpha_i',\beta_i')$ where

$$\alpha_i'=\alpha_i+\mathbf{z}\cdot\mathbf{e}_i\,, \tag{26}$$

$$\beta_i'=\beta_i+\mathbf{z}'\cdot\mathbf{e}_{\langle i\rangle} \tag{27}$$

for all i, where $\mathbf{z}$ and $\mathbf{z}'$ are independent arbitrary 3-vectors. We shall use the angular brackets to represent an operation on an integer argument n, ranging from 0 to 5, such that $\mathbf{e}_{\langle n\rangle}=\mathbf{e}_{(3n,\text{mod}5)}$ if $n\neq5$, and $\mathbf{e}_{\langle n\rangle}=-\mathbf{e}_n$ if $n=5$. The vectors $\mathbf{e}_i$ and $\mathbf{e}_{\langle i\rangle}$ are related to the two different 3D representations of the icosahedral group. The action of elements of the icosahedral group on the icosahedral star vectors, $\mathbf{e}_i$, is equivalent to a transformation of the following form: $\mathbf{e}_i\rightarrow\pm\mathbf{e}_{Pi}$, where Pi corresponds to a permutation of i's and the sign depends upon i and the particular group element. Thus, the icosahedral group can be represented by 6D matrices which act on the indices and change the signs of the $\mathbf{e}_i$'s. The 6D representation can be decomposed into two irreducible 3D representations, Γ_3 and Γ_3', which can be viewed as rotating the 3D vectors (rather than permuting the indices). The relationship between the $\mathbf{e}_i$ and $\mathbf{e}_{\langle i\rangle}$, then, is as follows: If an icosahedral group element has a representation in Γ_3 whose action on the $\mathbf{e}_i$ is equivalent to a permutation, $\mathbf{e}_i\rightarrow\pm\mathbf{e}_{Pi}$, then the same element has a representation in Γ_3' whose action is equivalent to a permutation, $\mathbf{e}_{\langle i\rangle}\rightarrow\pm\mathbf{e}_{\langle Pi\rangle}$ (where we have not specified the appropriate choices of signs). Note that our $\mathbf{e}_{\langle i\rangle}$ corresponds to $\mathbf{e}_i^{\perp}$ in Elser's papers[11] and $\mathbf{e}_i'$ in the papers of Duneau and Katz.[13]

Shifts of α_i of the form shown in Eq. (26) correspond to translations of the quasilattice equivalent to $\mathbf{x}\rightarrow\mathbf{x}-\mathbf{z}$ in Eq. (15). Such a shift results in $\psi_i\rightarrow\psi_i+(\mathbf{k}\cdot\mathbf{u}_{ijk})(\mathbf{z}\cdot\mathbf{e}_i)$ and the phase of the ijkth term in Eq. (20) is changed by

$$\mathbf{k}\cdot[(\mathbf{z}\cdot\mathbf{e}_i)\mathbf{u}_{ijk}+\text{cyclic permutations of }ijk]=\mathbf{k}\cdot\mathbf{z}, \tag{28}$$

where we have used the property of the $\mathbf{u}_{ijk}$'s, that $\mathbf{e}_i\cdot\mathbf{u}_{ijk}=1$ and $\mathbf{e}_j\cdot\mathbf{u}_{ijk}=\mathbf{e}_k\cdot\mathbf{u}_{ijk}=0$, to reduce the expression in square brackets to $\mathbf{z}$. From Eq. (28) we see that the change in phase of the ijkth term is independent of i, j, and k. Thus, the same phase change is made to each of the terms in Eq. (20) and the intensity of the peaks is not changed. Of course, an overall phase shift by $\mathbf{k}\cdot\mathbf{z}$ is just the change in $F_3(\mathbf{k})$ to be expected since Eq. (26) corresponds to a translation of the quasilattice by $\mathbf{z}$.

The shift of the β_i in Eq. (27) corresponds to a more subtle transformation of the lattice. In general, *the shift results in a rearrangement of the quasilattice grid planes in just such a way as to produce a new quasilattice that is locally isomorphic to the original.* (A much more thorough discussion of such transformations will be given in paper II.)

For each wave vector $\mathbf{k}$ in the reciprocal lattice there exists a unique $\mathbf{k}^u$ such that, if for some triplet $i\neq j\neq k$,

$$\mathbf{k}\cdot\mathbf{u}_{ijk}=k_{p_iq_i},\quad \mathbf{k}\cdot\mathbf{u}_{jki}=k_{p_jq_j},\quad\text{and }\mathbf{k}\cdot\mathbf{u}_{kij}=k_{p_kq_k}$$

where $k_{p_iq_i}$ is defined in Eq. (7)], then

$$\mathbf{k}^u\cdot\mathbf{u}_{\langle i\rangle\langle j\rangle\langle k\rangle}=2\pi q_i-\frac{k_{p_iq_i}}{\tau}\,, \tag{29}$$

plus two similar expressions with cyclic permutations of ijk. According to Eq. (25), then, a shift of the β_i of the form in Eq. (27) results in a shift

$$\psi_i\rightarrow\psi_i+\mathbf{k}^u\cdot\mathbf{u}_{\langle i\rangle\langle j\rangle\langle k\rangle}(\mathbf{z}'\cdot\mathbf{e}_{\langle i\rangle})\,,$$

resulting in a phase shift for the ijkth term in Eq. (20) of the form

$$\mathbf{k}^u\cdot[(\mathbf{z}'\cdot\mathbf{e}_{\langle i\rangle})\mathbf{u}_{\langle i\rangle\langle j\rangle\langle k\rangle}+\text{cyclic permutations of }ijk=\mathbf{k}^u\cdot\mathbf{z}', \tag{30}$$

where we have used the property that

$$\mathbf{e}_{\langle i\rangle}\cdot\mathbf{u}_{\langle i\rangle\langle j\rangle\langle k\rangle}=1$$

and

$$\mathbf{e}_{\langle j\rangle}\cdot\mathbf{u}_{\langle i\rangle\langle j\rangle\langle k\rangle}=\mathbf{e}_{\langle k\rangle}\cdot\mathbf{u}_{\langle i\rangle\langle j\rangle\langle k\rangle}=0\,.$$

Once again, we find that the net result of the shift is independent of i, j, and k. Therefore, each of the terms in the sum in Eq. (20) is changed by the same phase factor, $\exp(i\mathbf{k}^u\cdot\mathbf{z}')$, which can be brought out of the sum as an overall phase shift of $F_3(\mathbf{k})$. Thus, there is no change in the intensities of the peaks.

It is straightforward to show that Eqs. (26) and (27), in addition to rotations and inversions, represent the most general shifts in the (α_i,β_i) that leave the intensities of the diffraction pattern invariant. The results also apply to the rhombohedral unit-cell packings since any such packing is the decoration of some quasilattice [although, strictly speaking, our results have only been established for a class of quasilattices with flat planes and with spacings given by Eq. (1)]. In principle, the generalization to quasilattices with different symmetries only requires further application of group theory and vector analysis.

B. Physical significance of local isomorphism

In general, even for fixed orientational symmetry, quasiperiodicity, and unit-cell shapes, there are infinitely many distinct LI classes [corresponding, for example, to shifts in the (α_i,β_i) which are not of the form shown in Eqs. (26) and (27)]. No such issue arises for the case of periodic crystals where there is a unique configuration of cells—a single LI class containing one element. In Sec. IV A, we argued that two quasilattices (or packings) have diffraction patterns with identical intensities if and only if they are locally isomorphic. This result suggests some further physical consequences:

(i) Whereas modulations in the Bragg peak intensities for ideal crystals can be used to directly probe the atomic decorations of the unit cell, for quasicrystals the situation is more complicated. Modulations in intensity can be obtained not only by changing the atomic decorations of the (two or more) unit cells, but also by changing from one LI class of unit-cell packings to another.

(ii) The density wave description is expressed in terms of the Fourier components of the density, and the expression for the Landau mean free energy is expressed in terms of these components. In general, the free energy depends on both the phases and magnitudes of the components. Since two quasilattices in the same LI class have

the same Fourier transform (except for a **k**-dependent phase shift), their free energy must be the same (an overall phase shift such as obtained by a translation, does not change the free energy). By the same token, two quasilattices in different LI classes have different free energies, unless there is some accidental degeneracy. As support for this conclusion, note that in Ref. 17 it was shown that the density wave expansion for the Landau mean free energy of the icosahedral quasicrystal is invariant under phase shifts in the density waves (Fourier components) that correspond precisely to Eqs. (26) and (27).

(iii) Given this conjecture, if the ground state of some physical system is a quasicrystal state, as determined by minimizing the Landau mean free energy, then it is degenerate and corresponds to a set of configurations in a *single LI class* (neglecting the possibility of accidental degeneracy). For example, configurations corresponding to the quasicrystal packings that obey the matching rules described in Sec. II G have a different energy than configurations that do not obey the matching rules since, as we noted, they necessarily belong to different LI classes. The Penrose LI class of packings for any given symmetry (i.e., packings for which there exist matching and deflation rules) appears to be the simplest class for which conditions can be "rigged" (e.g., by covalent atomic or molecular bonding rules) so that quasicrystals in that class correspond to the ground state. We do not suggest, though, that this must be the case for *I*-Al-Mn in which there are metallic bond forces with nearly spherical symmetry.

(iv) The entropy of the ground state is determined by the number of energetically equivalent configurations. According to the arguments above, only configurations in the same LI class should be counted. Counting all possible rearrangements of the unit cells consistent with the quasiperiodicity and symmetry leads to a vast overestimate of the entropy.

V. COMPUTER MODELING AND THE STABILITY OF QUASICRYSTALS

Thus far, we have discussed only the unit-cell structure of ideal quasicrystals. In this section we discuss some of our work on computer modeling of atomic quasicrystals obtained by decorating the unit cells, including studies of stability.

One method of studying the stability of quasicrystals is to study the Landau mean free energy expressed as an expansion in density waves (cut off to include only the first few terms) and then to examine the stability of quasicrystals with the variation of parameters.[12,15,17,18,51] Although this is a powerful approach to such problems, the method has the disadvantage that there are many free parameters (Nelson and Sachdev have attempted to improve upon the method by utilizing experimental data to obtain fits to the values of the free parameters[18]) and the validity of cutting off the Landau expansion is questionable.

As an alternative approach to studying the stability of quasicrystals and to gaining better insight into possible realistic atomic quasicrystal structures, we initiated an extensive program using computer modeling of ideal atoms. This program began well before the report on *I*-Al-Mn (Ref. 6) appeared as an effort to find physical systems that might be likely candidates for forming quasicrystals. The goal was to find whether there existed any conditions for which the quasicrystal atomic configuration might be locally, or perhaps even globally, favored energetically. Obviously, this approach has its own limitations—sample size, relaxation time, etc.—but it serves as an interesting complement to the other methods. The most complete results to date are on 2D pentagonal atomic quasicrystals, which we shall discuss here, although some of the insights undoubtedly carry over to 3D structures as well.

One set of models is based on ideal atoms modeled as soft spheres interacting through Lennard-Jones interactions:

$$V_{\mathrm{LJ}}(r)=\epsilon\left[-\frac{1}{6}\left[\frac{r}{\sigma}\right]^{-6}+\frac{1}{12}\left[\frac{r}{\sigma}\right]^{-12}\right]. \tag{31}$$

where $V_{\mathrm{LJ}}(r)$ is the Lennard-Jones potential energy associated with two atoms separated by distance r.[4] The energy $\epsilon/12$ corresponds to the binding energy for a pair of atoms at the ideal separation, $r=\sigma$, both expressed in arbitrary units. The models contain two or more different atomic species. Associated with each possible pair of different species is a different set of parameters, (ϵ,σ), which is supposed to model the two-body interaction. These parameters may be chosen to favor different local atomic configurations. Our strategy was to find parameters that favor local fivefold symmetry, as described below.

For each model, the values of σ for two of the atomic species were chosen so that, after relaxation under the Lennard-Jones potential, five of the atoms of larger radius just fit around a central atom of smaller radius. In the hard-sphere limit, this means

$$r_1/r_2=\sin(\pi/5)/[1-\sin(\pi/5)]$$

so that five of the spheres with radius r_1 can densely pack around a central sphere with radius r_2 in a pentagonally symmetric configuration. This condition is chosen to alleviate the local frustration (on the scale of atomic clusters) so that inhibits the formation of pentagonal packings of identical atoms. Our notion was that, if the bond between the two different atoms is very strong, the formation of pentagonal clusters and then possibly pentagonal quasicrystals might be favored. Obviously, this notion is quite vague and we certainly do not argue that such a condition is required. (Nevertheless, it is intriguing that *I*-Al-Mn contains two atomic species such that, according to the effective atomic radii measured in metals, 12 aluminum atoms can fit densely around a central manganese atom.)

Next, we considered the possible atomic decorations of the Penrose lattice. Even for fixed ratios of the atomic radii, we found a wide range of possible stoichiometries. For the case of binary systems, for example, models have been constructed with stoichiometry (large:small) ranging from τ:1 to 5:1 with comparable packing fractions. In all the cases we constructed, there are vacant regions and two-level systems (ambiguities in the placement of atoms that contribute to the entropy).

All the examples we constructed were statically relaxed

using a conjugate gradient program to test the local stability of the atomic configuration.[25] In Fig. 11 we show an example of a ternary alloy decoration of a Penrose tiling after static relaxation. The initial configuration was a decoration of a Penrose tiling. The two types of decagons (arrangements of five fat and five skinny tiles) were each decorated with the large and medium size atoms. The smallest atoms were added to fill in the gaps that remained. Where two decagons overlap, only one could be decorated with a large atom. This binary choice is arbitrary (a kind of two-level system) and does not affect the relaxation. Although there is some decay of the orientational and translational symmetry after relaxation, the structure remains highly ordered. For example, we computed the orientational order parameters—

$$Q_n \equiv \langle \exp(in\theta) \rangle ,$$

where θ is the orientation angle of a bond joining two near-neighbor atoms measured with respect to some fixed axes and the angular brackets signify the average over all nearest-neighbor (as determined, say, by the Voronoi construction[3]) atomic bonds. In the unrelaxed configuration, Q_n is zero for $n < 10$ but Q_{10} is unity, indicating that the structure has perfect long-range pentagonal (or decagonal) orientational order. (Note that, since atomic bonds have orientations but not directions, $Q_n = 0$ for odd n; by this definition pentagonal and decagonal orientational order are equivalent.) For the relaxed configuration, the Q_n remain negligibly small for $n < 10$ and Q_{10} ranges between 0.5 and 0.95, depending on the model (each sample had 750 atoms or more). ($Q_{10} = 0.95$ for the example in Fig. 11.) To see if the decay in order is exponential, we computed the correlation function,

$$G_n(r) \equiv \langle Q_n(r) Q_n(0) \rangle ,$$

as a function of r and then determined the ratio $G_{10}(r)/G_0(r)$ to measure the decagonal orientational correlations;[25] the ratio decreased rapidly for small r but then appeared to reach a long plateau, indicating that the orientational order remained long range even after relaxation.

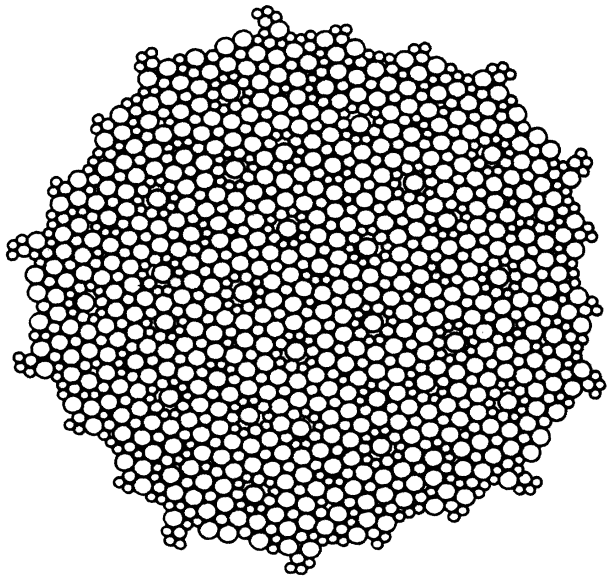

FIG. 11. Two-dimensional sphere packing using three different size spheres (a ternary alloy) which has been statically relaxed under a Lennard-Jones potential. This packing displays long-range pentagonal bond-orientational order, and, as may be seen by viewing at a grazing angle, sequences of parallel lines separated by 1 or τ (in suitable units) which indicate long-range quasiperiodic translational order. The initial (unrelaxed) configuration of atoms was a decoration of a Penrose tiling.

One interesting example is a binary alloy composed of a large (L) and small (S) atom such that (ϵ,σ) is (1.0,2.618) for the L-S interaction, (0.01,4.0) for the L-L interaction, and (0.01,2.8) for the S-S interaction. This case is designed so that the binding force between the two different atoms is much stronger than that between like atoms to greatly favor pentagonal clusters. (It seems peculiar at first that the value of σ for the S-S interaction is greater than for the L-S interaction. However, given that the value of ϵ is much greater for the L-S interaction, the separation after relaxation is greater for L-S than for S-S.) In Fig. 12, we show the bond-angle—bond-angle correlation function, $G_{10}(r)/G_0(r)$ suitably normalized, and the radial distribution function (RDF) of the relaxed structure, both of which illustrate that orientational and translational order is maintained over the sample. For this case, we have been able to find no crystalline phase that has lower energy, including numerous phase-separated crystalline states one might consider. Although this analysis is far from conclusive, it suggests that there may exist conditions under which the quasicrystal phase is even more energetically favorable than the crystalline state. This is consistent with the conclusions drawn from the analysis of the Landau theory.[12,15,17,18,51]

In three dimensions the only difference is that the steric hindrance to the formation of quasicrystals appears to be less than in two dimensions for all the models we have considered. For example, although there are cracks formed in a 3D packing of regular dodecahedra (since they do not pack crystallographically), the cracks represent a considerably smaller vacant volume than their analogues in a 2D packing of pentagons. Thus, we conclude that dense atomic quasicrystal structures are feasible; some may even be globally stable.

Since the Lennard-Jones parameters we studied were not realistic (that is, did not correspond to the values of the parameters found for the inert gases or metallic glasses), we next modeled a system that we hoped could be measured experimentally—a configuration of polystyrene spheres (polyballs) in colloidal suspension in an ionic solution interacting through electric and ionic forces. We modeled the polyball spheres using an interpolyball potential of the form:[57]

$$V = V_A + V_R \tag{32}$$

where V_A is the attractive van der Waals interaction and V_R is the repulsive double-layer interaction. V_A is given by

$$V_A = -\frac{H}{3}\left[\frac{1}{y^2+4y} + \frac{1}{(y+2)^2} + \tfrac{1}{2}\ln\left[\frac{y^2+4y}{(y+2)^2}\right]\right], \tag{33}$$

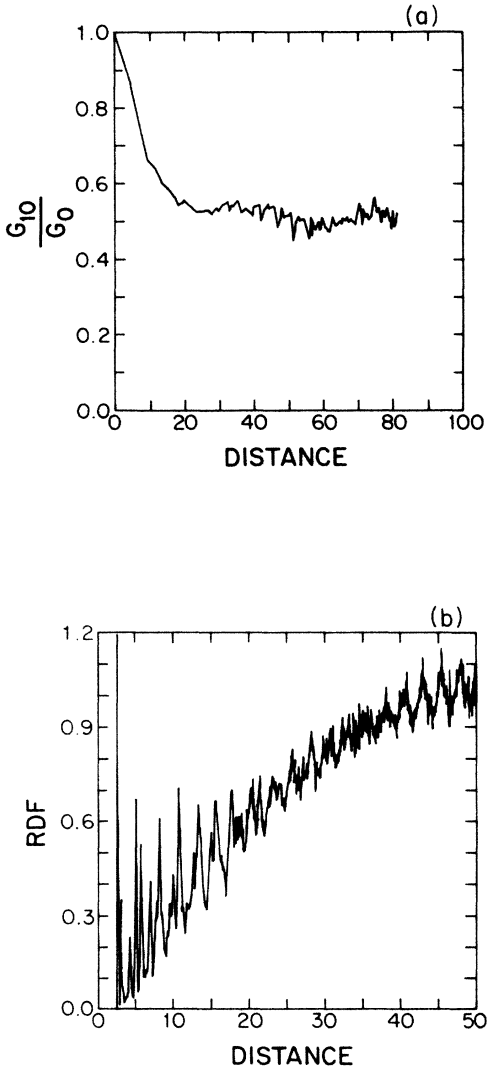

FIG. 12. (a) Bond-angle—bond-angle correlation function $G_{10}(r)/G_0(r)$ of the relaxed ternary "alloy" (2D sphere packing) normalized so that the function is unity for $r=0$. The alloy contains three types of atoms (large, medium, and small). Shown here is the bond-angle correlation for large atoms only, but correlations for medium and small atoms are similar. Note that the function drops sharply initially, but then levels off and oscillates about a value of approximately 0.5. (b) Radial distribution function (RDF) of the relaxed ternary alloy displaying the persistence of long-range translational order.

where y is the surface-to-surface distance divided by a; a is the sum of the radii of the two interacting polyballs; and H is the Hamaker constant for the system, typically of order $2\times10^{-20}J$. V_R was taken to be of the form:

$$V_R=\frac{\epsilon_r a\psi^2}{2}\ln[1+\exp(-\kappa a y)], \tag{34}$$

where $\epsilon_r=8.9\times10^{-9}$ C/V m is the dielectric constant of the medium; κ is the reciprocal Debye-Huckel reciprocal screening length; and ψ is the surface (double-layer) potential, for which a typical value is 0.1 V.[57]

The polyball system seems ideal, in principle, for finding quasicrystal configurations since so many physical parameters can be adjusted to produce optimal conditions for quasicrystal formation. For example, in two dimensions we can imagine a system composed of two polyball species with opposite charges such that five of the larger species just fit around a central smaller one after relaxation under the interpolyball potential. The force between different (oppositely charged) polyballs is much greater than the force between like polyballs due simply to electrostatic repulsion. Phase separation of the species or other simple crystal-like configurations appear to be highly suppressed energetically. (Of course, it is always very difficult to rule out the possibility of a periodic lattice with a very large unit cell.) According to our computer computations, for the choice of parameters above, a pentagonal quasicrystal configuration of spheres of radius $r_1=0.31$ μm and $r_2=0.33$ μm is at least locally stable under relaxation, and, by our argument above, possibly even globally favored energetically.

Unfortunately, one problem with testing this possibility in the laboratory is that oppositely charged polyballs tend to flocculate, forming large clumps before they can be mixed homogeneously. However, if the ionic concentration is kept high during mixing to screen the charges, and then the ionic concentration is rapidly changed to the desired value above, this problem might be overcome.[58]

VI. CONCLUSIONS

Quasicrystals are a well-defined ordered phase of solid matter with long-range quasiperiodic translational order and long-range orientational order. Because they are not periodic, they can have orientational symmetries disallowed for crystals; in fact, they can have arbitrary orientational symmetries corresponding to any star of symmetry vectors. They are characterized by a diffraction pattern composed of a dense set of true Bragg peaks in an array that reflects the orientational symmetry.

Quasicrystals can be classified by their orientational symmetry and quasiperiodicity (that is, the irrational numbers that determine the ratio of length scales). For fixed orientational symmetry, there are various manifestations of the same orientational symmetry, such as the vertex, edge, face, etc. models in the case of icosahedral orientational symmetry. In addition, for a given symmetry and quasiperiodicity, there exist many distinct local isomorphism classes of structures, where two structures are said to be locally isomorphic if and only if every finite region in each occurs identically somewhere in the other. If two structures have the same orientational symmetry and quasiperiodicity but are in different local isomorphism classes, they will have different Bragg peak intensities and Landau mean free energies. Therefore, a state with fixed energy, e.g., the ground state, corresponds to a single local isomorphism class.

Computer modeling of atomic quasicrystals and Landau theoretic treatments indicate that quasicrystal structures can be locally, and perhaps even globally stable ener-

getically. A range of stoichiometries appear to be locally stable.

A given system may exhibit phase transitions between quasicrystal structures with many different orientational symmetries or between two different manifestations of the same orientational symmetry, such as a transition from an icosahedral vertex model structure to an icosahedral face model.

The electron diffraction patterns of *I*-Al-Mn and related alloys clearly show that their structures are closely related to icosahedral quasicrystals; the positions of the diffraction peaks agree remarkably well with the predictions for an icosahedral quasicrystal. The electron micrographs, x-ray diffraction measurements, and the morphology of *I*-Al-Mn also appear to support the hypothesis that *I*-Al-Mn is an example of an icosahedral quasicrystal.

On the other hand, it should be noted that, although measurements of the orientational correlation length indicate that it is on the order of microns, all measurements of the translational correlation length are on the order of hundreds of angstroms.[59] The prejudice is that this is due to strain or to a high density of defects. If so, it might be expected that such defects can be annealed out in some samples (although it is much more difficult to anneal defects in quasicrystals compared to crystals[16,52]). Another possibility is that the *I*-Al-Mn structure is not really a quasicrystal, but an icosahedratic as described in Ref. 26. Such a structure has long-range orientational order and short-range translational order. It should also be noted that by considering larger and larger unit cells, a periodic crystal can be constructed so as to produce a diffraction pattern that arbitrarily well approximates a quasicrystal pattern. (A simple way to illustrate this is to take a single Penrose rhombus tile, deflate it arbitrarily many times, and then use the tile as a large unit cell for a periodic lattice.)

Whatever the case of *I*-Al-Mn, it is nevertheless apparent that a whole class of new atomic structures for solids is possible corresponding to a new phase of matter with unique symmetries and physical properties. Traditional concepts, such as the impossibility of fivefold symmetry, must be abandoned. We remain hopeful that nature will take frequent advantage of such an intriguing possibility.

The existence, both theoretically and experimentally, of icosahedral quasicrystals may also have ramifications for the study of glass structure, the subject that was the original motivation for this research. As we noted in Sec. II A, one of the leading models of metallic glass structure, discussed by Sadoc, Sethna, Nelson, and others,[26] is that over extended but finite length scales the glass is a structure with icosahedral orientational order. According to the model, the atomic arrangement in a metallic glass over *short distances* can be described as a projection from a packing of atoms that lie in a closed (spherical) curved manifold. The atoms in the curved manifold are packed in a perfect tetrahedral lattice in which 20 tetrahedra join at a point to form an icosahedron. The model is based on the notion that, although an icosahedral configuration of atoms is energetically favored on small scales, as was first noted by Frank,[60] the icosahedral symmetry of an atomic structure cannot be extended over a long range. The projection from curved space to flat space necessarily gives rise to disclination defects which disorder the orientational symmetry.

The quasicrystal is a counterexample to the notion that perfect icosahedral orientational symmetry is only possible on a curved manifold and that icosahedral orientational symmetry in flat space must be limited in range due to the presence of disclination defects. The loophole is that disclination defects may be so ordered and so dense in a structure that their effect on the long-range orientational order is screened and the icosahedral orientational order can be extended to infinite range. The resulting structure is then best regarded as a new kind of ideal ordered structure. Not only is this a theoretical possibility, as illustrated by our construction of icosahedral quasicrystal unit-cell packings, but also we have now an experiment involving a real metallic alloy system that exhibits long-range icosahedral orientational symmetry (extending over microns). The alloy was even produced by a splat-cooling process usually used to produce metallic glasses.

Of course, we take care to note that, even if the original motivations for the curved space projection model are shaken, it may still be a correct description of some, if not all, metallic glass structures. Using the model, computations of the structure factor for metallic glass have been obtained which appear to be reasonable,[26] although we do not know if the results depend only on the presence of small icosahedral clusters, which might be obtained with other models, or actually require the projection from curved manifolds.

Our own point of view continues to be that the metallic glass structure is closely related to that of the icosahedral quasicrystal. One possibility is that the structure and properties of a metallic glass are similar to those of an icosahedral quasicrystal with a high density of defects. Alternatively, it may be that there is a whole progression of periodic (crystalline), then quasiperiodic (quasicrystalline), and finally chaotic (glassy) structures that form a sequence of spatial possibilities analogous to the progression of periodic, quasiperiodic, and finally, chaotic behavior that form a sequence of temporal possibilities for dynamical systems. The state achieved by a given system would depend upon the kinetics by which the atoms sample the quasicrystal and crystal structural possibilities under the conditions of rapid quenching. This kind of approach might lead, we hope, to a unified theory of the atomic structures of solids.

ACKNOWLEDGMENTS

We wish to thank J. Socolar for this extensive advice during the preparation of the manuscript. We have also benefited from useful discussions with E. Bombieri, J. Cahn, P. Chaudhari, J. Conway, D. Coppersmith, T. Egami, V. Elser, D. Fisher, D. Gratias, P. Heiney, C. Henley, P. Horn, S. Kim, T. Lubensky, D. Nelson, S. Ostlund, P. Pleasants, S. Ramaswamy, J. Taylor, and J. Toner; and we thank B. Grunbaum for forwarding a portion

of his book manuscript to us prior to its publication. We wish to especially thank R. Amado and P. Chaudhari for their support and advice throughout this research project. This work was supported in part by the National Science Foundation Materials Research Laboratories (NSF-MRL) program under Grant No. DMR-82-16718, by the Department of Energy under Grant No. DOE-EY-76-C-02-3071, and by the Alfred P. Sloan Foundation. P.J.S. is grateful for the hospitality and financial support from the IBM Thomas J. Watson Research Laboratory and the Institute for Advanced Study in Princeton, where much of this research was completed.

---

[1]The terms crystal and crystallographic will refer, in this paper, only to periodic crystals.

[2]R. L. E. Schwarzenberger, *N-Dimensional Crystallography* (Pitman, London, 1980).

[3]N. W. Ashcroft and N. D. Mermin, *Solid State Physics* (Holt, Rinehart, and Winston, New York, 1976).

[4]See, for example, C. A. Angell, J. H. Clarke, and L. V. Woodcock, in *Advances in Chemical Physics,* edited by I. Progogine and S. Rice (Wiley, New York, 1981), Vol. 48, p.397.

[5]D. Levine and P. J. Steinhardt, Phys. Rev. Lett. **53**, 2477 (1984).

[6]D. S. Shechtman, I. Blech, D. Gratias, and J. W. Cahn, Phys. Rev. Lett. **53**, 1951 (1984).

[7]R. D. Field and H. L. Fraser, Mater. Sci. Eng. **68**, L17 (1984-85).

[8]M. Kuriyama, G. G. Long, and L. Bendersky, Phys. Rev. Lett. **55**, 849 (1985).

[9]L. Pauling, Nature **317**, 512 (1985).

[10]P. Kramer and R. Neri, Acta Crystallogr. Sect. A **40**, 580 (1984).

[11]V. Elser, Acta Crystallogr. Sect. A **42**, 36 (1986); Phys. Rev. B **32**, 4892 (1985).

[12]P. A. Kalugin, A. Kitaev. and L. Levitov, Pis'ma Zh. Eksp. Teor. Fiz. **41**, 119 (1985) [JETP Lett. **41**, 145 (1985)]; J. Phys. (Paris) **46**, L601 (1985).

[13]M. Duneau and A. Katz, Phys. Rev. Lett. **54**, 2688 (1985); J. Phys. (Paris) Colloq. **8**, 31 (1985).

[14]D. Mercier and J. C. S. Levy, Phys. Rev. B **27**, 77 (1983).

[15]P. Bak, Phys. Rev. Lett. **54**, 1517 (1985); Phys. Rev. B **32**, 5764 (1985). See also, the earlier work by S. Alexander and A. McTague, Phys. Rev. Lett. **41**, 702 (1978).

[16]D. Levine, T. C. Lubensky, S. Ostlund, S. Ramaswamy, P. J. Steinhardt, and J. Toner, Phys. Rev. Lett. **54**, 1520 (1985); T. C. Lubensky, S. Ramaswamy, and J. Toner, Phys. Rev. B **32**, 7444 (1985).

[17]N. D. Mermin and S. M. Troian, Phys. Rev. Lett. **54**, 1524 (1985); M. V. Jaric, *ibid.* **55**, 607 (1985).

[18]D. R. Nelson and S. Sachdev, Phys. Rev. B **32**, 689 (1985); **32**, 4592 (1985).

[19]J. E. S. Socolar, P. J. Steinhardt, and D. Levine, Phys. Rev. B **32**, 5547 (1985).

[20]N. de Bruijn, Ned. Akad. Weten. Proc. Ser. A **43**, 39 (1981); **43**, 53 (1981).

[21]F. Gahler and J. Rhyner, J. Phys. A **19**, 267 (1985). Note that these authors have discussed only periodic N-grids, whereas, in the previous reference, duals of quasiperiodic N-grids are also considered.

[22]J. E. S. Socolar and P. J. Steinhardt, following paper, Phys. Rev. B **34**, 617 (1986).

[23]Many groups have obtained high-resolution electron micrographs of the I-Al-Mn icosahedral phase, including R. Portier, D. Shechtman, D. Gratias, and J. W. Cahn, J. Electron. Microsc. **10**, 107 (1985); K. Hiraga, M. Hirabayashi, A. Inoue, and T. Masumoto, Sci. Rep. Res. Inst. Tohoku Univ. Ser. A **32**, 309 (1985); L. Bursill and J. Lin, Nature **316**, 50 (1985); K. Chattopadhyav, S. Ranganathan, G. N. Subbanna, and N. Thangaraj, Scr. Met. **19**, 767 (1985); K. M. Knowles, A. L. Greer, W. O. Saxton, and W. M. Stobbs, Philos. Mag. B **52**, L31 (1985); R. Gronsky and L. Tanner (unpublished).

[24]R. Penrose, Bull. Inst. Math. Appl. **10**, 266 (1974).

[25]P. J. Steinhardt, D. R. Nelson, and M. Ronchetti, Phys. Rev. Lett. **47**, 1297 (1981); Phys. Rev. B **28**, 784 (1983).

[26]D. R. Nelson, Phys. Rev. Lett. **50**, 982 (1983); Phys. Rev. B **28**, 5515 (1983). See also, J.-F. Sadoc, J. Phys. (Paris) Colloq. **41**, C8-326 (1980); J. P. Sethna, Phys. Rev. Lett. **50**, 2198 (1983).

[27]F. C. Frank and J. Kasper, Acta Crystallogr. **11**, 184 (1958); **12**, 483 (1959).

[28]P. Chaudhari and P. J. Steinhardt, in *Amorphous Materials: Modeling of Structure and Properties,* edited by V. Vitek (AIME, New York, 1982), p. 239.

[29]M. Gardner, Sci. Am. **236** (1), 110 (1977).

[30]T. Ishimasa, H.-U. Nissen, and Y. Fukano, Phys. Rev. Lett. **55**, 511 (1985).

[31]L. Bendersky, Phys. Rev. Lett. **55**, 1461 (1985).

[32]For a review, see P. Bak, Rep. Prog. Phys. **45**, 587 (1981). V. L. Pokrovsky and A. L. Talapov, *Theory of Incommensurate Crystals,* Soviet Science Reviews (Harwood Academic, Chur, Switzerland, 1985).

[33]General properties of a set of points that satisfy the minimal separation condition are discussed by R. V. Galiulin, Kristallografiya **25**, 901 (1980) [Sov. Phys.—Cryst. **25**, 517 (1980)]. Such sets of points are refered to as Delaunay systems.

[34]For a discussion of the properties of quasiperiodic functions see A. S. Besicovitch, *Almost Periodic Functions* (Cambridge, London, 1932).

[35]In. Ref. 13, the authors suggested that our construction requires a center of symmetry. Although there are exceptional cases (a set of measure zero) with centers of symmetry, in general a center of symmetry is *not* required.

[36]This is a larger class of 2D possibilities than was suggested in Ref. 5. We thank E. Bombieri and J. Taylor (private communication) for explaining many properties of algebraic numbers that made it clear that any regular polygon can satisfy the constraints necessary to generate a 2D quasicrystal. Bombieri (unpublished) has also proven important properties about the diffraction patterns for general 1D quasicrystals.

[37]Note that even though the projection constructions do not refer explicitly to self-similarity, deflation rules or self-similarity transformations do exist for the resulting structures. See paper II or discussion by V. Elser, *ibid.*; or P. Pleasants (Ref. 38).

[38]P. Pleasants, Banach Number Theory Center Publications (unpublished).

[39]We thank R. Amado and P. Chaikin for suggesting the moiré pattern construction.

[40]B. Grunbaum and G. C. Shepard, *Tilings and Patterns* (Freeman, San Fransisco, in press). R. Ammann and J. H. Conway have discovered numerous interesting properties of the Penrose tilings. Ammann has not published his results, but he has communicated them in brief notes to Conway and M. Gardner, who were kind enough to share the information with us. Also, many of Ammann's and Conway's results and conjectures are found in Grunbaum and Shephard's forthcoming book. Ammann's suggestion for 3D tiles is discussed in A. L. Mackay's papers.

[41]G. J. Janusz, *Algebraic Number Fields* (Academic, New York, 1973).

[42]V. Hoggatt, *Fibonacci and Lucas Numbers* (Houghton Mifflin Co., Boston, 1969).

[43]L. M. Corliss, J. M. Hastings, and R. J. Weiss, Phys. Rev. Lett. **3**, 211 (1959); V. N. Bykov, V. S. Kolovkin, N. V. Ageev, and V. A. Levdik, Doklady Akad. Nauk SSSR **128**, 1153 (1959) [Sov. Phys.—Dokl. **4**, 1070 (1960)].

[44]The field generated by an algebraic number z is $Q[z]$ (reads Q adjoins z), where Q denotes the set of rational numbers. $Q[z]$, the smallest field containing the rational numbers and z, consists of all numbers of the form $\sum_{j=0}^{n-1} q_j z^j$ where $q_j \in Q$.

[45]S. Kim and J. E. S. Socolar (unpublished).

[46]H. S. M. Coxeter, *Regular Polytopes,* 3rd ed. (Dover, New York, 1973), p. 26.

[47]D. Levine and P. Steinhardt, University of Pennsylvania Patent Disclosures, UPENN-84-06 (1983) and M-1516 (1984) (unpublished).

[48]A. Mackay, Kristallografiya **26**, 910 (1981) [Sov. Phys.—Cryst. **26**, 517 (1982)]; Physica **114A**, 609 (1982).

[49]P. Kramer Acta Crystallogr. Sect. A **38**, 257 (1982).

[50]R. Mosseri and J. F. Sadoc, in *Structure of Non-Crystalline Materials, 1982* (Taylor and Francis, London, 1983), p. 137.

[51]T.-L. Ho, Phys. Rev. Lett. **56**, 468 (1985).

[52]T. C. Lubensky, S. Ramaswamy, and J. Toner, Phys. Rev. B **32**, 7444 (1985).

[53]P. Bak, Phys. Rev. B **32**, 5764 (1985).

[54]R. K. P. Zia and W. J. Dallas, J. Phys. A **18**, L341 (1985).

[55]S. Ostlund (private communication); see also, J. Cahn, D. Shechtman, and D. Gratias (unpublished).

[56]We thank D. R. Nelson (private communication) for first emphasizing for us the importance of the (2×2)-fold plane.

[57]C. A. Castillo, R. Rajagopalan, and C. S. Hirtzel, Rev. Chem. Eng. **2**, 237 (1984).

[58]P. Chaudhari (private communication).

[59]P. Bancel, P. A. Heiney, P. W. Stephens, A. I. Goldman, and P. M. Horn, Phys. Rev. Lett. **54**, 2422 (1985).

[60]F. C. Frank, Proc. R. Soc. London, Ser. A **215**, 43 (1952).

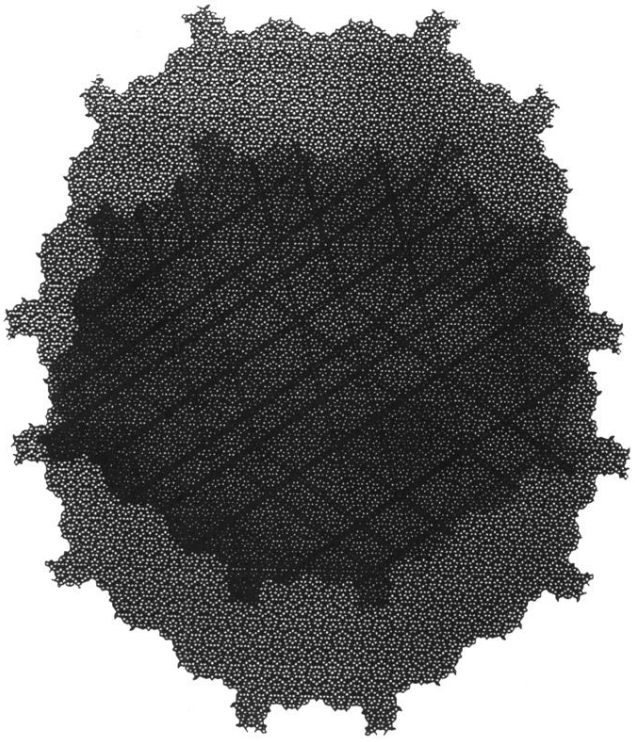

FIG. 3. Two identical Penrose tilings, one translated with respect to the other, are overlayed to form a moiré pattern. Where the two patterns interfere constructively or destructively, light or dark lines appear.

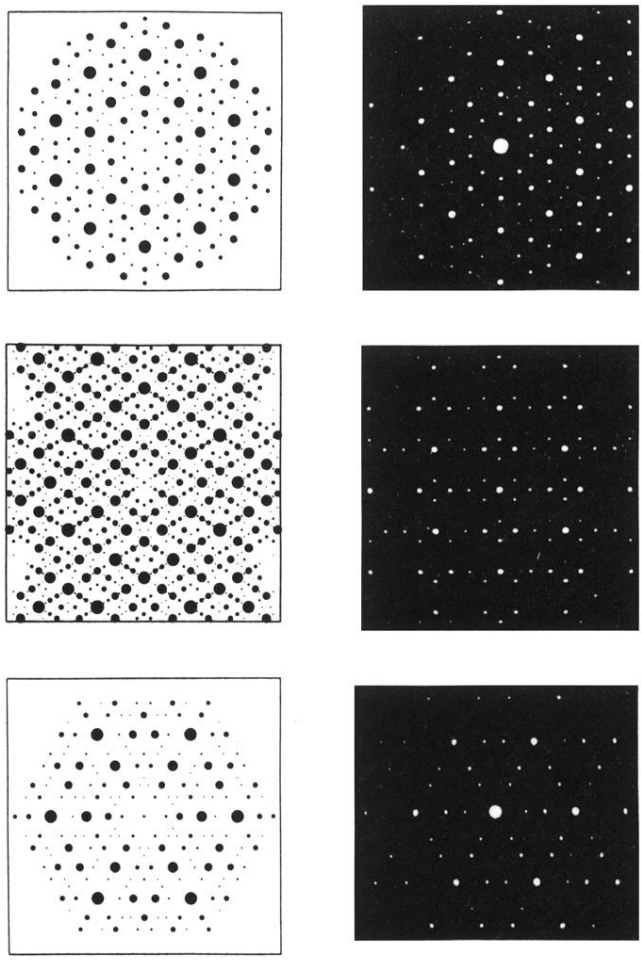

FIG. 9. Computed diffraction patterns of the icosahedral Ammann plane quasilattice (left) and the experimental electron diffraction patterns taken on a rapidly cooled alloy of aluminum manganese. (a) In a plane normal to a fivefold axis of an icosahedron. (b) In a plane normal to a threefold axis. (c) In a plane normal to a (2×2)-fold axis.